Title

Nerve-associated transient receptor potential ion channels can contribute to intrinsic resistance to bacterial adhesion in vivo

Journal

The FASEB Journal, 35(10)

ISSN

0892-6638

Authors

Wan, Stephanie J
Datta, Ananya
Flandrin, Orneika
et al.

Publication Date

2021-10-01

DOI

10.1096/fj.202100874r

Peer reviewed

HHS Public Access

Author manuscript

FASEB J. Author manuscript; available in PMC 2022 October 01.

Published in final edited form as:

FASEB J. 2021 October ; 35(10): e21899. doi:10.1096/fj.202100874R.

Nerve-associated transient receptor potential ion channels can contribute to intrinsic resistance to bacterial adhesion *in vivo*

Stephanie J Wan[*], **Ananya Datta**[†], **Orneika Flandrin**[*], **Matteo ME Metruccio**[†], **Sophia Ma**[†], **Vincent Nieto**[†], **Abby R Kroken**[†], **Rose Z. Hill**[#], **Diana M. Bautista**[#], **David J Evans**[†,‡], **Suzanne MJ Fleiszig**[*,†,§,1]

[*]Vision Science Program, University of California, Berkeley, CA USA

[†] School of Optometry, University of California, Berkeley, CA USA

[#] Department of Molecular and Cell Biology and Helen Wills Neuroscience Institute, University of California, Berkeley, CA USA

[‡] College of Pharmacy, Touro University California, Vallejo, CA USA

[§] Graduate Groups in Microbiology and Infectious Diseases & Immunity, University of California, Berkeley, CA USA

Abstract

The cornea of the eye differs from other mucosal surfaces in that it lacks a viable bacterial microbiome and by its unusually high density of sensory nerve endings. Here, we explored the role of corneal nerves in preventing bacterial adhesion. Pharmacological and genetic methods were used to inhibit the function of corneal sensory nerves or their associated transient receptor potential cation channels TRPA1 and TRPV1. Impacts on bacterial adhesion, resident immune cells, and epithelial integrity were examined using fluorescent labeling and quantitative confocal imaging. TRPA1/TRPV1 double gene-knockout mice were more susceptible to adhesion of environmental bacteria and to that of deliberately-inoculated *Pseudomonas aeruginosa*. Supporting the involvement of TRPA1/TRPV1-expressing corneal nerves, *P. aeruginosa* adhesion was also promoted by treatment with bupivacaine, or ablation of TRPA1/TRPV1-expressing nerves using RTX. Moreover, TRPA1/TRPV1-dependent defense was abolished by enucleation which severs corneal nerves. High-resolution imaging showed normal corneal ultrastructure and surface-labeling by wheat-germ agglutinin for TRPA1/TRPV1 knockout murine corneas, and intact barrier function by absence of fluorescein staining. *P. aeruginosa* adhering to corneas after perturbation of nerve or TRPA1/TRPV1 function failed to penetrate the surface. Single gene-knockout mice showed roles for both TRPA1 and TRPV1, with TRPA1$^{-/-}$ more susceptible to *P. aeruginosa* adhesion while TRPV1$^{-/-}$ corneas instead accumulated environmental bacteria. Corneal CD45+/CD11c+ cell responses to *P. aeruginosa* challenge, previously shown to counter bacterial adhesion, also depended on TRPA1/TRPV1 and sensory nerves. Together, these results demonstrate roles for

[1]Correspondence: Dr. Suzanne M. J. Fleiszig, School of Optometry, University of California, Berkeley, CA 94720 USA. Tel. 1 (510) 643-0990, fleiszig@berkeley.edu.

Author contributions

S. J. Wan, A. Datta, O. Flandrin, M. M. E. Metruccio, S. Ma, V. Nieto and R. Z. Hill conducted the experiments. All authors contributed to the data analysis. S. J. Wan, A. R. Kroken, R. Z. Hill, D. M. Bautista, D. J. Evans and S. M. J. Fleiszig wrote the manuscript. S. J. Wan, D. M. Bautista, D. J. Evans and S. M. J. Fleiszig were responsible for research design.

corneal nerves and TRPA1/TRPV1 in corneal resistance to bacterial adhesion *in vivo* and suggest that the mechanisms involve resident immune cell populations.

Keywords

TRP ion channels; Sensory nerves; Epithelial defense; Bacterial adhesion; Cornea

Introduction

While the cornea of the eye is routinely exposed to environmental debris, pathogens, and allergens, it differs from other exposed tissue surfaces by lacking a stable viable bacterial microbiome (1). This resistance is effective enough to rapidly clear even large inocula of the potential pathogens *Pseudomonas aeruginosa* and *Staphylococcus aureus* (1–3). In contrast to the intact cornea, corneal epithelial cells are exquisitely sensitive to bacterial adhesion and virulence mechanisms when cultured *in vitro* (4–7), underscoring the importance of *in vivo* factors in modulating the outcome of bacterial challenge.

The mucosal (tear) fluid bathing the corneal surface plays critical roles in this regard. Similar to other mucosal fluids, tear fluid contains an array of antimicrobial factors such as lactoferrin, lysozyme, and transferrin, in addition to β-defensins, cathelicidins and keratin-derived antimicrobial peptides (8–13). Our published data have shown directly that tear fluid can protect *in vitro* grown corneal epithelial cells against the potential pathogen *P. aeruginosa,* and that this translates to protection *in vivo* (3, 11, 14, 15). We further showed that its protective mechanisms extend beyond direct antimicrobial activity. Tear fluid inhibits *P. aeruginosa* twitching motility, a property critical for virulence by this opportunist (11, 16), dependent on the tear fluid ingredient DMBT1, also present in saliva (11, 17). Tear fluid can also act directly on the host epithelial cells to enhance their resistance to bacterial virulence (18), correlating with numerous changes to epithelial cell gene expression, with specific upregulated factors (e.g. RNase7, ST-2) and microRNA regulation involved in the mechanisms (19). Tear fluid treatment of corneal epithelial cells grown as multilayers increases their transepithelial resistance and reduces their susceptibility to traversal by *P. aeruginosa* (15), suggesting that integrity of tight junctions and/or normal cell sorting critical to cell polarity and barrier function are involved, properties that confer appropriate localization of surface associated mucins, and all of which contribute to epithelial defense against *P. aeruginosa* (7, 20–23). Tear fluid, which contains over 700 biologically active proteins, glycoproteins and lipids, is likely to exert these activities *via* receptors critical to the epithelial-intrinsic defenses against *P. aeruginosa in vivo,* which include MyD88, IL-1R and/or TLRs (1, 20–24).

In vivo factors other than tear fluid can also modulate the susceptibility of corneal epithelial cells to *P. aeruginosa*. They include the basement membrane (basal lamina) that lies below the epithelium. Indeed, *in vitro* multilayers of corneal epithelial cells display enhanced resistance to traversal by *P. aeruginosa* if grown on a protein substrate mimicking the basal lamina *in vivo*, and correlating with a general enhancement of transepithelial resistance (28). Another *in vivo* contributor to countering bacterial adhesion to the epithelial surface is the

rapid CD11c+/dendritic cell response that occurs in the absence of overt inflammation if an infection-resistant cornea is challenged with *P. aeruginosa* (29).

Despite this progress, it remains unclear why the corneal lacks a microbiome. The adjacent conjunctiva, also exposed to the surface and therefore also bathed in tear fluid, is routinely colonized by *Corynebacterium* sp. and other non-pathogenic Gram-positive bacteria (30–32). Further, the conjunctiva has even more ready access to CD11c+ cells and other components of immunity, being armed with its own associated lymphoid tissue, blood vessels and a rich supply of goblet cells - all absent from the immune-privileged cornea.

Another major difference between cornea and conjunctiva is in their distribution of sensory nerves. While the conjunctiva is sparsely innervated, the density of sensory nerves endings in the cornea exceeds all other tissue in the body (33–35). The potential for sensory nerve involvement in the cornea's intrinsic defense against bacteria was suggested by results of our previous study in which we reported that healthy murine corneas respond to bacterial challenge by mounting a CD11C+/dendritic cell response (29). In that study, we found the response to be surprisingly rapid and to be absent after enucleation (29), a process that separates the sensory nerve endings from their cell bodies residing in the trigeminal ganglion of the brain (33, 34).

In the cornea, the majority of the nerve fibers are polymodal (70%), and thus able to respond to a wide range of stimuli including mechanical, thermal, and chemical cues. These responses involve polymodal transient receptor potential (TRP) cation channels, the majority being TRPV1 (Vanilloid) with TRPA1 (Ankyrin) expressed on a subset of TRPV1-expressing C-fiber polymodal sensory neurons. Triggering these channels initiates sensory transduction (34, 36, 37), and can also cause the local release of neuropeptides thereby inciting or exacerbating inflammatory responses (38, 39). In the corneal epithelium, the neuropeptides released include Substance P, Calcitonin Gene-Related Peptide (CGRP) and Glial cell line-derived neurotrophic factor Family Receptor alpha3 (GFRα3) (38), with GFRα3 expressed in the superficial layers of the corneal epithelium instead of CGRP. Neuropeptides can have both direct and indirect impacts on other cell types in the vicinity of the nerve endings, including epithelial and immune cells, which can in turn modulate inflammatory responses (34, 40, 41). This involves receptors for neuromodulators on immune cells, including dendritic cells and neutrophils (42). Not surprisingly, resident immune cells (both dendritic and macrophages) in the cornea have been found in close proximity to nerve fibers (43, 44) with functional significance for corneal physiology and homeostasis (33, 34, 37).

Both TRPV1 and TRPA1 have been associated with the detection of noxious stimuli and the development and modulation of inflammation in numerous different tissues and disease states (38). For example, TRPA1 was shown to mediate inflammation in animal models of dermatitis, colitis, and asthma (45–47). An additional and expanding area of interest, however, is the role of TRP-expressing sensory neurons in detecting microbial ligands (antigens) and modulating host inflammatory and immune defenses to infection (48). TRPA1 can be directly activated by bacterial components such as LPS (49, 50) and pain associated with *S. aureus* infections *in vivo* was shown to involve direct nociceptor

activation involving the pore-forming toxin α-hemolysin and bacterial N-formylated peptides (51). During *S. aureus* pneumonia, TRPV1-expressing sensory neurons modulate neutrophil and γδ T cell responses thereby promoting infection severity (52). Similarly, during *Streptococcus pyogenes* necrotizing fasciitis, bacterial toxin-mediated release of CGRP also suppressed neutrophil responses to promote bacterial survival (42). It was also more recently shown that during *P. aeruginosa* infection of the cornea, inflammation is promoted by TRPV1, associated with CGRP-mediated recruitment of neutrophils with reduced bactericidal activity (53). Clearly, the role(s) of TRPA1 and TRPV1 nociceptors in modulating progression of infection and associated disease pathology via immune cell recruitment/function is complex and further studies will help elucidate tissue and/or pathogen specificity of their involvement.

The ability of TRP channels to directly respond to microbial ligands in milliseconds would also make them an ideal first line of defense against pathogens. TRPV1-expressing sensory neurons help defend the GI tract against *Salmonella enterica* (serovar Typhimurium) adhesion, invasion and dissemination *via* release of CGRP to promote protective levels of resident commensal bacteria (54). However, less is known regarding the participation of TRP-expressing sensory nerves in the intrinsic barrier function of other mucosal epithelia against microbes during health, a function that is especially important for the cornea of the eye for which clarity is essential for vision.

In this study, we explored the roles of corneal sensory nerves and TRP nociceptors in corneal epithelial resistance to bacterial adhesion using multiple methods to inhibit their activities. The results showed contributions for nerve fibers, TRPA1 and TRPV1. While only TRPA1 was required to defend the cornea against *P. aeruginosa* adhesion during health and after superficial injury, TRPV1 was instead required to prevent adhesion to the healthy murine cornea of environmental bacteria. Shedding light on the mechanisms involved, corneal nerves and TRPA1/TRPV1 were found to modulate CD45+ and CD11c+ corneal responses to bacterial inoculation, the latter previously shown to counter bacterial adhesion to superficially-injured corneas *in vivo* (29).

MATERIALS AND METHODS

Bacteria

Pseudomonas aeruginosa strain PAO1 expressing dTomato on plasmid p67T1 (PAO1-dtom) (55) was used throughout the study. Inocula were prepared from overnight cultures grown on tryptic soy agar plates supplemented with carbenicillin 400 μg/mL at 37 °C for ~16 h. Bacteria were then suspended in Dulbecco's Modified Eagle's Medium (DMEM) (Lonsa, Walkersville,MD) to a concentration of ~10^{11} CFU/mL measured by spectrophotometry and concentrations confirmed by viable counts.

Murine models of bacterial adhesion

All procedures were carried out in accordance with standards established by the Association for the Research in Vision and Ophthalmology, under the protocol AUP-2016–08-9021 approved by the Animal Care and Use Committee, University of California Berkeley, an

AAALAC accredited institution. The protocol adheres to PHS policy on the humane care and use of laboratory animals, and the guide for the care and use of laboratory animals. Six to twelve week old male or female homozygous TRPA1$^{-/-}$/TRPV1$^{-/-}$ [double gene knockout mice] and homozygous TRPV1$^{-/-}$ or TRPA1$^{-/-}$ [single gene knockout mice; (56, 57)] in the C57BL/6 background were used along with age and sex-matched wild-type controls. In some experiments CD11c-yfp transgenic wild-type mice were used to visualize CD11c+ cells (yellow) or *mT/mG* mice were used to visualize all cell membranes (red) (29).

The *in vivo* model of bacterial adhesion was used as described previously (29). Mice were anesthetized by intraperitoneal injection of ketamine (80–100 mg/Kg) and dexmedetomidine (0.25–0.5 mg/Kg). Corneas were rinsed with PBS to wash away tear fluid. In one group, one cornea was subjected to blotting with a Kimwipe™ tissue paper to enable bacterial adhesion. Eyes were inoculated with 5 μL of *P. aeruginosa* (~10^{11} CFU/mL) once every hour for 4 h while under sustained anesthesia. After 4 h, animals were euthanized by a further intraperitoneal injection of ketamine (80–100 mg/Kg) and xylazine (5–10mg/Kg) followed by cervical dislocation. Eyes were enucleated, rinsed with PBS, and fixed in 2 % paraformaldehyde (PFA) overnight at 4 °C, then imaged using confocal microscopy with a 60x [or 20x] water-dipping objective.

For *ex vivo* experiments, mice were euthanized as above without prior interventions, eyes were enucleated and washed in PBS to exclude tear fluid. Some eyes were blotted with a Kimwipe™ as above then all eyes were placed in a 200 μL suspension of *P. aeruginosa* (~10^{11} CFU/mL) in a 96-well plate and incubated for 4 h at 37 °C. Eyes were then washed in PBS and imaged as above. Bacteria were identified and quantified by ImageJ on maximum intensity projections (reducing a 3D image into a 2D image by projecting the maximum intensity of each pixel to the z plane).

Fluorescence *in Situ* Hybridization (FISH)

Labeling of bacteria on murine corneas without prior manipulation was performed as previously described (1). Briefly, mice were euthanized as above, eyes enucleated and fixed in 2 % PFA for 1 h with rotation at room temperature (RT). Fixed eyes were then washed in 80 % EtOH, 95 % EtOH, and then PBS for 10 min each at RT. Eyes were placed in hybridization buffer solution [NaCl (0.9 M), Tris-HCl (20 mM, pH 7.2) and SDS (0.01 %)] and incubated at 55 °C for 30 min and then the 16S rRNA gene probe below was added to a final concentration of 100 nM and incubated at 55 °C overnight. Bacterial hybridization was performed using the universal 16S rRNA gene [Alexa488]-GCTGCCTCCCGTAGGAGT-[Alexa488] (Eurofins Genomics) (58, 59). Eyes were then transferred to wash buffer solution [NaCl (0.9 M) and Tris-HCl (20 mM, pH 7.2)] and washed three times for 10 min each at RT before imaging on confocal microscope using a 60x [or 20x] water-dipping objective. Bacteria were identified and quantified by ImageJ on maximum intensity projections.

Ablation of TRPA1 and TRPV1 sensory nerves

TRPA1 and TRPV1 expressing cells were selectively ablated using subcutaneous chronic application of RTX as previously described (60, 61). One milligram of RTX was dissolved

in 500 μL 96 % ethanol and diluted in sterile PBS. Mice were anesthetized with isoflurane and then RTX injected subcutaneously at 20 μg/Kg body weight daily for 3 days. Control mice were injected with PBS. To confirm ablation of TRPA1 and TRPV1 in the cornea, the eye wipe test was performed in lightly anesthetized animals. Briefly, capsaicin solution (100 μM) was dropped into the eye and the number of defensive wiping movements for 1 min was counted. To image CD11c+ cells, a 20x water-dipping objective was used and images quantified with ImageJ.

Wheat Germ Agglutinin (WGA) labeling

Mice were anesthetized and one eye inoculated with bacteria as described above. After 4 h, mice were euthanized, eyes enucleated and rinsed in PBS. Eyes were then transferred to Alex Fluor® 647 conjugate of wheat germ agglutinin solution (10 μg/mL, Invitrogen™) for 5 min at RT then washed 3 times with PBS. Eyes were then fixed in 2 % PFA overnight at 4 °C before imaging using confocal microscopy with a 60x water-dipping objective. Mean fluorescence intensity and area covered on maximum intensity projections were quantified using ImageJ.

Fluorescein staining

After induction of anesthesia, eyes were rinsed with PBS and stained with fluorescein as previously described (1). Briefly, for wild-type mice, one eye was blotted with a Kimwipe™ tissue paper as a positive control. A 5 μL drop of fluorescein solution (0.02 %) was then added to the ocular surface and corneal epithelial integrity examined using a slit lamp and confocal microscopy with a 60x water-dipping objective. Mean fluorescence intensity and area covered on maximum intensity projections were quantified using ImageJ.

Corneal nerve block

To suppress neuronal activation in the cornea, 0.5 % bupivacaine solution (62, 63) was injected (5 μL) subconjuntivally in anesthetized mice with a Hamilton small volume syringe and small hub 33 gauge needle. Then, 5 μL was topically applied onto the cornea. After 20 min, corneas were washed with PBS and bacterial inoculation performed as described above.

Confocal microscopy

Murine eyeballs were imaged *ex vivo* as previously described (24). Eyes were fixed to a 12 mm glass coverslip with cyanoacrylate glue with cornea facing upward. The coverslip with eyeball was placed in 46 mm Petri dish and filled with PBS to cover the eyeball completely. Confocal imaging was performed using an Olympus FV1000 confocal microscope [Olympus BX615Wi upright microscope with Olympus FluoView 1000 detection system equipped with Laser Diodes (LD) 405, 440, 559, 635 and an Argon Laser 488/515]. The 488 nm laser used for detection of bacteria labeled with FISH, corneas stained with fluorescein, 515 nm laser for CD11c-yfp, the 559 nm laser was used for detection of red-fluorescent bacteria (PAO1-dtom) or red fluorescent cell membranes, and the 635 nm laser for corneas stained with WGA or CD45+ antibody. In instances where red-fluorescent cell membrane mice were not used, ocular surface reflectance (excitation and emission at same wavelength) was obtained. For 60x images, four or more randomly

chosen fields of each eye were imaged from the corneal surface. For 20x images, three or more randomly chosen fields of each eye were imaged from the corneal surface. Three-dimensional images were reconstructed from z-stacks using IMARIS software (Bitplane).

Statistical Analysis

Statistical analysis was performed using Prism (GraphPad Software, Inc.). Data were expressed as mean ± standard error of the mean (SEM). Statistical significance of differences between means was determined using Student's *t*-Test for two group comparisons or one- or two-way ANOVA with Tukey's multiple comparisons test for three or more groups. For nonparametric data, the Mann-Whitney U test was used for two group comparisons or the Kruskal-Wallis test for three or more groups. P values of less than 0.05 were considered significant. All experiments were repeated at least once.

RESULTS

Corneas of TRPA1$^{-/-}$/TRPV1$^{-/-}$ mice are more susceptible to adhesion of environmental bacteria and inoculated *P. aeruginosa*

To determine if TRPA1 and/or TRPV1 are involved in preventing bacterial adhesion (microbiome) formation on the healthy corneal surface, untreated corneas of wild-type mice were compared to TRPA1$^{-/-}$/TRPV1$^{-/-}$ mice for presence of resident bacteria. For this purpose, FISH labeling *in situ* was done using a universal 16S rRNA gene probe to detect bacteria (1). Results revealed ~4-fold more bacteria present on corneas of TRPA1$^{-/-}$/TRPV1$^{-/-}$ mice versus wild-type (Fig. 1), suggesting that one or both contribute to preventing adhesion of environmental bacteria.

We next asked if the cornea's intrinsic resistance to potential pathogens also requires either of these proteins. Thus, corneas of wild-type and TRPA1$^{-/-}$/TRPV1$^{-/-}$ mice were challenged with *P. aeruginosa in vivo* using previously described methods (29). Some corneas were challenged without prior manipulation (healthy), others were superficially-injured by gently blotting the epithelium with a KimWipe™ before inoculation (21, 24). Previously, we showed that this blotting process increases the propensity for bacteria to attach to the corneal surface, causes removal/death of superficial epithelial cells, increases epithelial permeability to fluorescein, but does not allow bacteria to penetrate the epithelium and cause infection (21, 24, 29, 64). Results showed that with and without tissue paper-blotting, TRPA1$^{-/-}$/TRPV1$^{-/-}$ corneas were more susceptible to *P. aeruginosa* adhesion than wild-type corneas (~2.2-fold and ~3.1-fold, respectively) (Fig. 2A, B). Irrespective of whether or not blotting was done prior to inoculation, bacteria adhering to the corneas of TRPA1$^{-/-}$/TRPV1$^{-/-}$ mice did not penetrate beyond the corneal surface (Fig. 2C) showing that defenses that operate after adhesion were not compromised in these mice.

To further test the role of TRPA1 and TRPV1 neurons in bacterial adhesion we used a pharmacological approach. RTX, a highly potent TRPV1 agonist, was utilized to ablate neurons expressing TRPV1 from wild-type mice (60, 61). This treatment also ablates the subset of nerves that co-express both TRPV1 and TRPA1. To confirm successful ablation of TRPV1 nociceptors, the capsaicin eye wipe test showed that mice treated with RTX did

not exhibit the paw wiping behavior demonstrated by vehicle control mice after topical capsaicin application on the eye (Fig. 2D). Aligning with results obtained with TRPA1$^{-/-}$/TRPV1$^{-/-}$ mice, RTX-treated mice had an increased propensity to bind *P. aeruginosa* for both healthy (no blot) and blotted (superficially-injured) corneas (~3.7-fold and ~4.7-fold, respectively) (Fig. 2F, G).

TRPA1$^{-/-}$/TRPV1$^{-/-}$ impacts on bacterial adhesion are abolished after enucleation of the eye (*ex vivo*) or suppressing nerve function *in vivo* using the local anesthetic bupivacaine

Enucleation of the eye separates the nerve endings in the cornea from their cell bodies which reside in the trigeminal ganglion. Thus, experiments were performed *ex vivo* as an additional method for considering the role of nerves and TRPA1$^{-/-}$/TRPV1$^{-/-}$. Immediately after enucleation, corneas of wild-type and TRPA1$^{-/-}$/TRPV1$^{-/-}$ mice were inoculated with *P. aeruginosa* with or without prior blotting. Results from *ex vivo* eyes contrasted with the above *in vivo* findings by showing no significant difference in *P. aeruginosa* adhesion between wild-type and TRPA1$^{-/-}$/TRPV1$^{-/-}$ corneas for healthy (no blot) and blotted (superficially-injured) conditions (Fig. 3A, B). Controls showed, as expected, an increased susceptibility to *P. aeruginosa* adhesion after blotting occurred both *in vivo and ex vivo* (Fig. 2A, B and Fig. 3A, B respectively) (21, 24, 29). While providing more support for the involvement of TRPA1$^{-/-}$/TRPV1$^{-/-}$ on corneal nerves in the mechanisms by which the healthy cornea resists bacterial adhesion, these results also show that some defenses against adhesion compromised by superficial injury are independent of regulation by intact corneal nerves.

Next, we returned to the *in vivo* model and blocked the function of all peripheral nerves using a subconjunctival injection of 0.5% bupivacaine hydrochloride (bupivacaine), a local anesthetic. Controls confirmed that bupivacaine effectively reduced corneal sensitivity to capsaicin (Fig. 3C). Epithelial integrity was also maintained as shown by resistance to fluorescein staining after corneas were treated (Fig. 3D). Bupivacaine-treated corneas showed a significant increase in *P. aeruginosa* adhesion after *in vivo* challenge with *P. aeruginosa* compared to vehicle controls under both healthy (~3.6-fold) and blotted conditions (~3.5-fold) (Fig. 3E, F).

Epithelial integrity in TRPA1$^{-/-}$/TRPV1$^{-/-}$ mice is similar to wild-type

To begin exploring mechanisms by which TRPA1$^{-/-}$/TRPV1$^{-/-}$ contribute to preventing bacterial adhesion, we next examined their importance for maintaining epithelial integrity. A second reason to study epithelial integrity was to explore if corneal epithelial cells express functional TRPV1 (65), in which case mutants lacking TRPV1 and RTX-treated corneas would be expected to have epithelial abnormalities, with RTX potentially damaging any cell expressing functional TRPV1 (60).

Fluorescein staining provides a useful indicator for disruption of epithelial tight junctions or damage to the epithelial surface (21, 24). Thus, corneas of wild-type and TRPA1$^{-/-}$/TRPV1$^{-/-}$ mice were compared for propensity to stain with fluorescein as evaluated using slit lamp examination. Blotted wild-type corneas were used as a positive control. As expected, fluorescein staining was observed on blotted, but not healthy (no blot)

wild-type corneas. Staining was also absent on healthy (no blot) TRPA1$^{-/-}$/TRPV1$^{-/-}$ corneas, which appeared morphologically similar to wild-type (Fig. 4A). To rule out subtle morphological differences, confocal imaging was used, also allowing the data to be quantified. Results again showed significant fluorescein penetration only in blotted corneas (Fig. 4A). Interestingly, when fluorescence intensity was quantified (Fig. 4B), the data showed even less fluorescence for TRPA1$^{-/-}$/TRPV1$^{-/-}$ corneas compared to wild-type corneas, although this was not statistically significant. Providing additional evidence that corneal epithelial integrity did not depend on TRPV1/TRPA1, and also showing that functional TRPV1 is lacking from the corneal epithelium, corneas of RTX-treated mice appeared normal and did not stain with fluorescein (Fig 2E).

To further explore impact on epithelial cells, TRPA1$^{-/-}$/TRPV1$^{-/-}$ mouse corneas were compared to wild-type for labeling with fluorescent-conjugated wheat germ agglutinin (WGA). WGA binds to N-acetyl glycosamine and sialic acids. Thus, it can be used to delineate apical cell morphology, labeling components of the ocular surface glycocalyx, which is the membrane-associated mucin barrier that can function to protect the corneal epithelium from microbes and other potential threats (66–69). Without blotting or bacterial challenge, results showed WGA labeling patterns similar for wild-type and TRPA1$^{-/-}$/TRPV1$^{-/-}$ mice (Fig. 5A). This was confirmed by quantification of mean fluorescence intensity and area of labeling covered (Fig. 5B). *P. aeruginosa* challenge had no significant effect on WGA labeling for either wild-type or TRPA1$^{-/-}$/TRPV1$^{-/-}$ mutants (Fig. 5A, B).

Collectively, these results suggest that corneas lacking both TRPA1 and TRPV1 maintain significant epithelial or tight junctional integrity.

CD45+ and CD11c+ immune cell responses to *P. aeruginosa* also depend on TRPA1/TRPV1

When healthy or blotted mouse corneas are challenged with *P. aeruginosa*, a rapid CD11c+ (dendritic) cell response occurs (29). If the cornea is blotted to induce superficial injury before inoculation, this response protects the cornea against bacterial adhesion. The rapidity of this CD11c+ response and its absence *ex vivo* led us to hypothesize dependence on corneal nerves, aligning with the known interdependence of corneal nerves and dendritic cells (43, 44).

TRPA1$^{-/-}$/TRPV1$^{-/-}$ mice were compared with wild-type for their CD45+ cell response after *P. aeruginosa* challenge. Bacterial inoculation of healthy corneas caused a significant increase in CD45+ cells that was absent in TRPA1$^{-/-}$/TRPV1$^{-/-}$ mice (Fig. 6A, B) showing that one or both of these TRP nociceptors were required for corneal leukocyte responses to bacterial inoculation.

Since TRPA1$^{-/-}$/TRPV1$^{-/-}$ mice with fluorescent immune cell reporters were not available, we next utilized (CD11c+-yfp transgenic) mice to allow more specific detection and quantification of corneal CD11c+ cells. RTX or bupivacaine were then used to study TRPA1/TRPV1 and sensory nerve involvement respectively. For healthy (no blot) corneas, RTX attenuated the normal CD11C+ cell response to *P. aeruginosa* challenge without a significant impact on baseline CD11C+ cell numbers in uninoculated eyes (Fig. 7A, B). Our previously published research showed that in addition to increasing the number of

CD11C+ cells, *P. aeruginosa* inoculation of the cornea also changed their morphology, significantly increasing perimeter measurements, reducing circularity and causing more dendritic projections, as confirmed by quantification (29). For RTX treated mice, these morphological changes did not occur after bacterial challenge (Fig. 7C). Similar results were obtained when corneas were superficially-injured by blotting before bacterial inoculation, in that RTX reduced the CD11C+ cell response in terms of cell numbers and eliminated changes to cell morphology (Fig. 7D, E, F). Bupivacaine treatment closely mimicked the effects of RTX in attenuating the CD11c+ cell response to *P. aeruginosa* in both healthy and superficially injured corneas (Fig. 7G). These results provide evidence that the observable CD11c+ cell responses occurring in *P. aeruginosa*-challenged corneas are also dependent on TRP-expressing sensory nerves. Given that this response can counter *P. aeruginosa* adhesion, it is likely to be a contributor to mechanisms by which corneal nerves/TRP-channels protect the cornea against adhesion of bacteria, its involvement being an intermediary step.

TRPA1 and TRPV1 both contribute to intrinsic corneal resistance to bacterial adhesion

Since TRPV1 has been shown to respond to bacterial components and to modulate immune responses during some infections, we next tested the hypothesis that TRPV1 rather than TRPA1 was responsible for preventing bacterial adhesion to the cornea. This was done using TRPV1$^{-/-}$ mice, which retain sensory nerve endings expressing TRPA1. The results showed no significant differences between wild-type and TRPV1$^{-/-}$ mice for healthy or blotted corneas in susceptibility to *P. aeruginosa* adhesion (Fig. 8A, B). Instead, TRPA1$^{-/-}$ corneas (able to express TRPV1) were more susceptible to *P. aeruginosa* adhesion compared to both wild-type and TRPV1$^{-/-}$ mice closely mirroring our findings with TRPA1$^{-/-}$/TRPV1$^{-/-}$ mice. This outcome occurred in both healthy and blotted corneas (Fig. 9A, B).

We next asked if TRPA1 also contributed to the intrinsic resistance of the murine cornea to adhesion of environmental bacteria (microbiome formation). Surprisingly, FISH labeling experiments showed mice lacking TRPA1 resembled wild-type in lacking adhesion of environmental bacteria (Fig. 10A, B). Instead, adhesion of environmentally-acquired bacteria was detected on TRPV1$^{-/-}$ mouse eyes, similar to TRPA1$^{-/-}$/TRPV1$^{-/-}$ mice. These results suggested that mechanisms driving intrinsic resistance of the cornea to adhesion of environmental bacteria differ from those protecting against *P. aeruginosa* adhesion by involving TRPV1 rather than TRPA1.

DISCUSSION

While previous studies have investigated the role of Transient Receptor Potential (TRP) cation channels in modulating infectious and inflammatory disease pathology, the data presented in this report show a novel role for TRP nociceptors in intrinsic defense during health. Here, we found that TRPA1 and TRPV1 associated with corneal nerves can contribute to intrinsic resistance to bacterial adhesion in mouse corneas using multiple methods, including use of; 1) TRPA1$^{-/-}$/TRPV1$^{-/-}$ knockout mice, 2) RTX to ablate sensory nerve endings expressing TRPV1 and co-expressed TRPA1, and 3) bupivacaine to block sensory nerve function. The results showed that these perturbations led to accumulation of environmental bacteria on the corneal surface, while also rendering healthy

and superficially-injured corneas less resistant to adhesion by the potential pathogen *P. aeruginosa*. Results from experiments using enucleated eyes or the local anesthetic bupivacaine to inhibit nerve function revealed that TRPA1/TRPV1-associated protection against bacterial adhesion to the cornea was nerve-dependent. Bacteria adhering to the corneal surface did not penetrate into the epithelium under any condition examined, even when there was pre-existing superficial injury. Loss of resistance to *P. aeruginosa* adhesion as a result of TRPA1/TRPV1 deficiency or suppression of nerve function was found to correlate with reduced CD45+ and CD11c+ cell responses to bacterial challenge, the latter previously shown to counter bacterial adhesion to superficially injured corneas.

The method used to induce superficial injury involved blotting the corneal surface with tissue paper. This procedure enhances susceptibility of the corneal epithelium to *P. aeruginosa* adhesion without allowing adherent bacteria to penetrate beyond the surface, a step required for infection to ensue (21). Our previous research has shown that blotting in this manner makes the cornea susceptible to fluorescein staining (a form of epithelial barrier function loss), removes corneal surface glycosylation, and damages residual surface cells (21, 24, 61). The results of the current study showed that blotted corneas, already more susceptible to *P. aeruginosa* adhesion, became even more susceptible when mice were TRPA1 deficient (+/− TRPV1 deficiency) or if nerve function was suppressed. That outcome suggests that TRPA1/nerve-dependent defenses against adhesion differ from those compromised by blotting. Indeed, corneas of $TRPA1^{-/-}/TRPV1^{-/-}$ mice, and those treated with RTX or bupivacaine, contrasted with blotted corneas by not displaying visible disruption to epithelial integrity, barrier function or surface glycosylation as shown by the absence of fluorescein staining, obvious morphological changes, or alterations to WGA-labeling. Separation of nerve/TRP-dependent defenses against *P. aeruginosa* from those compromised by blotting aligns with our previous work showing that blotting still enhances susceptibility to adhesion and traversal after enucleation, which severs nerves that innervate the cornea (21, 24, 29).

Our prior research has identified multiple factors that contribute to preventing epithelial traversal when *P. aeruginosa* is able to adhere to the corneal surface. They include TLR5, IL-1R, antimicrobial peptides, SP-D and other factors compromised by calcium chelation that probably include deeper layer cell-to-cell junctions (3, 21, 29). Given that multiple factors are able to counter traversal, there is likely be a significant amount of redundancy among them. Thus, a role for nerves/TRPA1 in defense against traversal cannot be ruled out by our results that showing lack of traversal when they are compromised.

In addition to increasing *P. aeruginosa* adhesion to corneas, TRPA1/TRPV1 deficiency or inhibiting nerve function also suppressed the infiltration of CD45+ and CD11c+ cells that otherwise occurred when mouse corneas were challenged with *P. aeruginosa*. Previously, we showed that the CD11c+ cell response can counter *P. aeruginosa* adhesion to mouse corneas (29). Together these findings suggests that intrinsic resistance to *P. aeruginosa* adhesion at the surface of the corneal epithelium involves communication between corneal sensory nerves and immune cells. A role for nerves in relaying information between the surface of the multilayered corneal epithelium to immune cells that reside deeper within the cornea aligns with the anatomy and known function of corneal nerves, that extend

to the epithelial surface and can quickly transfer information across significant distances. Other studies have shown that TRP channels on nerves can respond to various stimuli by releasing neuropeptides, including Substance P and CGRP, leading to an influx and activation of immune cells (38–40, 70, 71). TRP channels have also been shown able to directly sense bacterial components, causing release of immune mediators that modulate macrophages, dendritic cells, T lymphocytes and innate lymphoid cells (49–51). These published studies contribute to our understanding of how nerves interface with microbes and immune cells to drive inflammation during infection pathology. However, the present study instead aims to understand how the healthy, uninflamed cornea counters bacterial adhesion to resist infection, another topic with potential for development of novel infection management strategies. Disease pathogenesis and maintenance of health reflect opposite outcomes of bacterial challenge. While they appear to involve some overlapping factors, including sensory nerves and immune cells, the mechanistic details must differ. Thus, this area warrants separate investigation with experiments designed to ask different questions.

Use of homozygous single gene knockout mice showed distinct roles for TRPA1 and TRPV1 in countering bacterial adhesion, with TRPA1 reducing adhesion of *P. aeruginosa*, and TRPV1 instead hindering adhesion of environmental bacteria. This suggests that triggering of these distinct channels leads to different responses to modulate conditions at the epithelial surface, one that routinely hinders environmental microbes and the other only occasional to counter adhesion of a potential pathogen. The commensals around the mouse cornea deterred by TRPV1 are mostly Gram-positive and few in number, while the *P. aeruginosa* challenge we found to be countered by TRPA1 involves a Gram-negative potential pathogen introduced in much larger numbers. Thus, there are various possibilities for that specificity that will need to be deciphered, including commensal versus pathogen, Gram-type and inoculum size.

One difference between routine exposure to commensal bacteria and challenge with *P. aeruginosa* is that the latter induces an immune cell response above baseline. It is also possible that continued resistance to *P. aeruginosa* adhesion in the absence of TRPV1 is also influenced by their increased susceptibility to the adhesion of commensals. Moreover, hindering adhesion of different microbes might instead (or additionally) reflect that TRPA1 and TRPV1 appear to be triggered by different bacterial factors (49–51). More research will be required to determine the relative roles of TRPV1 and TRPA1 in modulating baseline and reactive immune cell responses during health, and consequences at the epithelial surface in the context of bacterial challenge.

Previously, we showed that ability of the cornea to resist adhesion of environmental bacteria depends on IL-1R and MyD88, associated with antimicrobial activity of corneal lysates, and that this is unaffected by induction of experimental dry eye (1, 25, 72). Research by us and others has shown that antimicrobial peptides constitute an important component of corneal defense against bacteria (8–10, 26, 73–76). Routinely-expressed antimicrobial peptides are potential candidates for mediating TRPV1-dependent prevention of commensal adhesion. However, TRPA1 activation might also alter antimicrobial peptide expression to more specifically target pathogens. It will be of value to explore if antimicrobial peptides

contribute to TRPA1 or TPV1 defense against bacterial adhesion and if so, the cell types involved in their expression.

There is controversy as to whether TRPV1 is expressed on cell types other than sensory neurons (77). Indeed, mRNA expression of TRPV channels and TRPV1-agonist responses have been reported in corneal epithelial cells *in vitro* (58). However, our findings showing that the corneal epithelium remains healthy after treatment with RTX, a potent TRPV1 agonist that damages cells expressing TRPV1 (60), suggests that functional versions of TRPV1 are not present on murine corneal epithelial cells *in vivo*, or that non-neuronal cells are less susceptible to calcium overload-induced death due to their non-excitable nature and lack of voltage-gated sodium and calcium channels. More research will be needed to understand the significance of our findings in the context of this earlier publication.

In conclusion, this study demonstrates a novel role for nerves in defending healthy *in vivo* epithelia against adhesion by both commensals and a potential pathogen. They further show the involvement of both TRPA1 and TRPV1, and that these two channels modulate activity against distinct bacterial types. In addition to contributing to our understanding of ocular surface homeostasis, these findings may also have implications in a clinical context in humans where local anesthetics are routinely applied to the ocular surface in optometric and ophthalmological settings. While this research raises many questions while answering a few, the results reveal a form of pattern recognition driven by sensory nerves to help direct appropriate responses to specific microbes at an epithelial surface that maintain homeostasis. In the murine cornea, this contributes to maintaining the absence of a microbiome and deterring the adhesion of potential pathogens. As technologies evolve, it may be possible to determine the extent to which these findings also apply to the human cornea. Furthermore, little is known about what determines microbiome composition at distinct locations within a host, only that they differ within and among hosts. Whether pattern recognition by sensory nerves and associated TRP channels participate in determining microbiome composition at body sites other than the cornea remains to be determined.

Acknowledgments

Funding sources: Supported by the National Eye Institute: EY011221 & EY030350 (SMJF)

Non-standard abbreviations

CFU	Colony Forming Units
CGRP	Calcitonin Gene-Related Peptide
DMBT1	Deleted in Malignant Brain Tumors 1
GFRα3	Glial cell line-derived neurotrophic factor Family Receptor alpha 3
IL-1R	Interleukin-1 Receptor
LPS	Lipopolysaccharide
MyD88	Myeloid Differentiation primary response gene 88

RNase7	RiboNuclease 7
RTX	Resiniferatoxin
TLR	Toll-Like Receptor
TRPA1	Transient Receptor Potential Ankyrin 1
TRPV1	Transient Receptor Potential Vanilloid 1
TSA	Tryptic Soy Agar
WGA	Wheat-germ agglutinin

References

1. Wan SJ, Sullivan AB, Shieh P, Metruccio MME, Evans DJ, Bertozzi CR, and Fleiszig SMJ (2018) IL-1R and MyD88 contribute to the absence of a bacterial microbiome on the healthy murine cornea. Front. Microbiol. 9, 1117 [PubMed: 29896179]
2. Mun JJ, Tam C, Kowbel D, Hawgood S, Barnett MJ, Evans DJ, and Fleiszig SMJ (2009) Clearance of *Pseudomonas aeruginosa* from a healthy ocular surface involves surfactant protein D and is compromised by bacterial elastase in a murine null-infection model. Infect. Immun. 77, 2392–2398 [PubMed: 19349424]
3. Augustin DK, Heimer SR, Tam C, Li WY, Le Due JM, Evans DJ, and Fleiszig SMJ (2011) Role of defensins in corneal epithelial barrier function against *Pseudomonas aeruginosa* traversal. Infect. Immun. 79, 595–605 [PubMed: 21115716]
4. Fleiszig SMJ, Zaidi TS, and Pier GB (1995) *Pseudomonas aeruginosa* invasion of and multiplication within corneal epithelial cells in vitro. Infect. Immun. 63, 4072–4077 [PubMed: 7558321]
5. Fleiszig SM, Wiener-Kronish JP, Miyazaki H, Vallas V, Mostov KE, Kanada D, Sawa T, Yen TS, and Frank DW (1997) *Pseudomonas aeruginosa*-mediated cytotoxicity and invasion correlate with distinct genotypes at the loci encoding exoenzyme S. Infect Immun 65, 579–586 [PubMed: 9009316]
6. Kroken AR, Chen CK, Evans DJ, Yahr TL, and Fleiszig SMJ (2018) The impact of ExoS on *Pseudomonas aeruginosa* internalization by epithelial cells is independent of *fleQ* and correlates with bistability of type three secretion system gene expression. MBio 9, e00668–18 [PubMed: 29717012]
7. Fleiszig SMJ, Evans DJ, Do N, Vallas V, Shin S, and Mostov KE (1997) Epithelial cell polarity affects susceptibility to *Pseudomonas aeruginosa* invasion and cytotoxicity. Infect. Immun. 65, 2861–2867 [PubMed: 9199460]
8. Mohammed I, Said DG, and Dua HS (2017) Human antimicrobial peptides in ocular surface defense. Prog. Retin. Eye Res. 61, 1–22 [PubMed: 28587935]
9. Redfern RL, Reins RY, and McDermott AM (2011) Toll-like receptor activation modulates antimicrobial peptide expression by ocular surface cells. Exp Eye Res 92, 209–220 [PubMed: 21195713]
10. Tam C, Mun JJ, Evans DJ, and Fleiszig SMJ (2012) Cytokeratins mediate epithelial innate defense through their antimicrobial properties. J. Clin. Invest. 122, 3665–3677 [PubMed: 23006328]
11. Li J, Metruccio MME, Evans DJ, and Fleiszig SMJ (2017) Mucosal fluid glycoprotein DMBT1 suppresses twitching motility and virulence of the opportunistic pathogen *Pseudomonas aeruginosa*. PLoS Pathog. 13, e1006392 [PubMed: 28489917]
12. McDermott AM (2013) Antimicrobial compounds in tears. Exp. Eye Res. 117, 53–61 [PubMed: 23880529]
13. Flanagan JL and Willcox MDP (2009) Role of lactoferrin in the tear film. Biochimie 91, 35–43 [PubMed: 18718499]

14. Fleiszig SMJ, Kwong MSF, and Evans DJ (2003) Modification of *Pseudomonas aeruginosa* interactions with corneal epithelial cells by human tear fluid. Infect. Immun. 71, 3866–3874 [PubMed: 12819071]
15. Kwong MSF, Evans DJ, Ni M, Cowell BA, and Fleiszig SMJ (2007) Human tear fluid protects against *Pseudomonas aeruginosa* keratitis in a murine experimental model. Infect. Immun. 75, 2325–2332 [PubMed: 17325054]
16. Zolfaghar I, Evans DJ, and Fleiszig SMJJ (2003) Twitching motility contributes to the role of pili in corneal infection caused by *Pseudomonas aeruginosa*. Infect. Immun. 71, 5389–5393 [PubMed: 12933890]
17. Li J, Wan SJ, Metruccio MME, Ma S, Nazmi K, Bikker FJ, Evans DJ, and Fleiszig SMJ (2019) DMBT1 inhibition of *Pseudomonas aeruginosa* twitching motility involves its N-glycosylation and cannot be conferred by the Scavenger Receptor Cysteine-Rich bacteria-binding peptide domain. Sci. Rep. 9, 13146 [PubMed: 31511582]
18. Mun JJ, Tam C, Evans DJ, and Fleiszig SMJJ (2011) Modulation of epithelial immunity by mucosal fluid. Sci. Rep. 1, 8 [PubMed: 22355527]
19. Mun J, Tam C, Chan G, Kim JH, Evans D, and Fleiszig S (2013) MicroRNA-762 is upregulated in human corneal epithelial cells in response to tear fluid and *Pseudomonas aeruginosa* antigens and negatively regulates the expression of host defense genes encoding RNase7 and ST2. PLoS One 8, e57850 [PubMed: 23469087]
20. Fleiszig SMJ, Zaidi TS, Ramphal R, and Pier GB (1994) Modulation of *Pseudomonas aeruginosa* adherence to the corneal surface by mucus. Infect. Immun. 62, 1799–1804 [PubMed: 8168942]
21. Alarcon I, Tam C, Mun JJ, le Due J, Evans DJ, and Fleiszig SMJ (2011) Factors impacting corneal epithelial barrier function against *Pseudomonas aeruginosa* traversal. Investig. Ophthalmol. Vis. Sci. 52, 1368–1377 [PubMed: 21051692]
22. Gipson IK, Spurr-Michaud S, Tisdale A, and Menon BB (2014) Comparison of the transmembrane mucins MUC1 and MUC16 in epithelial barrier function. PLoS One 9, e100393 [PubMed: 24968021]
23. Fleiszig SM, Vallas V, Jun CH, Mok L, Balkovetz DF, Roth MG, and Mostov KE (1998) Susceptibility of epithelial cells to *Pseudomonas aeruginosa* invasion and cytotoxicity is upregulated by hepatocyte growth factor. Infect. Immun. 66, 3443–3446 [PubMed: 9632620]
24. Tam C, LeDue J, Mun JJ, Herzmark P, Robey EA, Evans DJ, and Fleiszig SMJ (2011) 3D quantitative imaging of unprocessed live tissue reveals epithelial defense against bacterial adhesion and subsequent traversal requires MyD88. PLoS One 6, e24008 [PubMed: 21901151]
25. Sullivan AB, Connie Tam KP, Metruccio MME, Evans DJ, and Fleiszig SMJ (2015) The importance of the *Pseudomonas aeruginosa* type III secretion system in epithelium traversal depends upon conditions of host susceptibility. Infect. Immun. 83, 1629–1640 [PubMed: 25667266]
26. McDermott AM, Redfern RL, Zhang B, Pei Y, Huang L, and Proske RJ (2003) Defensin expression by the cornea: multiple signalling pathways mediate IL-1beta stimulation of hBD-2 expression by human corneal epithelial cells. Invest Ophthalmol Vis Sci 44, 1859–1865 [PubMed: 12714616]
27. Reins RY, Courson J, Lema C, and Redfern RL (2017) MyD88 contribution to ocular surface homeostasis. PLoS One 12, e0182153 [PubMed: 28796783]
28. Alarcon I, Kwan L, Yu C, Evans DJ, and Fleiszig SMJJ (2009) Role of the corneal epithelial basement membrane in ocular defense against *Pseudomonas aeruginosa*. Infect. Immun. 77, 3264–3271 [PubMed: 19506010]
29. Metruccio MME, Tam C, Evans DJ, Xie AL, Stern ME, and Fleiszig SMJ (2017) Contributions of MyD88-dependent receptors and CD11c-positive cells to corneal epithelial barrier function against *Pseudomonas aeruginosa*. Sci. Rep. 7, 13829 [PubMed: 29062042]
30. Fleiszig SMJ and Efron N (1992) Microbial flora in eyes of current and former contact lens wearers. J. Clin. Microbiol. 30, 1156–1161 [PubMed: 1583113]
31. Willcox MDP (2013) Characterization of the normal microbiota of the ocular surface. Exp. Eye Res. 117, 99–105 [PubMed: 23797046]

32. Ozkan J, Nielsen S, Diez-Vives C, Coroneo M, Thomas T, and Willcox M (2017) Temporal Stability and Composition of the Ocular Surface Microbiome. Sci. Rep. 7, 9880 [PubMed: 28852195]
33. Al-Aqaba MA, Dhillon VK, Mohammed I, Said DG, and Dua HS (2019) Corneal nerves in health and disease. Prog. Retin. Eye Res. 73, 100762 [PubMed: 31075321]
34. Belmonte C, Nichols JJ, Cox SM, Brock JA, Begley CG, Bereiter DA, Dartt DA, Galor A, Hamrah P, Ivanusic JJ, Jacobs DS, McNamara NA, Rosenblatt MI, Stapleton F, and Wolffsohn JS (2017) TFOS DEWS II pain and sensation report. Ocul. Surf. 15, 404–437 [PubMed: 28736339]
35. Müller LJ, Marfurt CF, Kruse F, and Tervo TMT (2003) Corneal nerves: structure, contents and function. Exp. Eye Res. 76, 521–542 [PubMed: 12697417]
36. Okada Y, Reinach PS, Shirai K, Kitano-Izutani A, Miyajima M, Yamanaka O, Sumioka T, and Saika S (2015) Transient receptor potential channels and corneal stromal inflammation. Cornea 34, Suppl 11 S136–141 [PubMed: 26448171]
37. Reinach PS, Mergler S, Okada Y, and Saika S (2015) Ocular transient receptor potential channel function in health and disease. BMC Ophthalmol. 15, Suppl 1 S153
38. Bautista DM, Pellegrino M, and Tsunozaki M (2012) TRPA1: A Gatekeeper for Inflammation. Annu. Rev. Physiol. 75, 181–200 [PubMed: 23020579]
39. Pinho-Ribeiro FA, Verri WA, and Chiu IM (2017) Nociceptor Sensory Neuron–Immune Interactions in Pain and Inflammation. Trends Immunol. 38, 5–19 [PubMed: 27793571]
40. Mantelli F, Micera A, Sacchetti M, and Bonini S (2010) Neurogenic inflammation of the ocular surface. Curr. Opin. Allergy Clin. Immunol. 10, 498–504 [PubMed: 20706114]
41. Mosimann BL, White MV, Hohman RJ, Goldrich MS, Kaulbach HC, and Kaliner MA (1993) Substance P, calcitonin gene-related peptide, and vasoactive intestinal peptide increase in nasal secretions after allergen challenge in atopic patients. J. Allergy Clin. Immunol. 92, 82–88 [PubMed: 8335859]
42. Pinho-Ribeiro FA, Baddal B, Haarsma R, O'Seaghdha M, Yang NJ, Blake KJ, Portley M, Verri WA, Dale JB, Wessels MR, and Chiu IM (2018) Blocking Neuronal Signaling to Immune Cells Treats Streptococcal Invasive Infection. Cell 173, 1083–1097.e22 [PubMed: 29754819]
43. Seyed-Razavi Y, Chinnery HR, and McMenamin PG (2014) A novel association between resident tissue macrophages and nerves in the peripheral stroma of the murine cornea. Investig. Ophthalmol. Vis. Sci. 55,1313–1320 [PubMed: 24458151]
44. Gao N, Lee P, and Yu FS (2016) In traepithelial dendritic cells and sensory nerves are structurally associated and functional interdependent in the cornea. Sci. Rep. 6, 36414 [PubMed: 27805041]
45. Caceres AI, Brackmann M, Elia MD, Bessac BF, del Camino D, D'Amours M, Witek JS, Fanger CM, Chong JA, Hayward NJ, Homer RJ, Cohn L, Huang X, Moran MM, and Jordt S-E (2009) A sensory neuronal ion channel essential for airway inflammation and hyperreactivity in asthma. Proc. Natl. Acad. Sci. 106, 9099–9104 [PubMed: 19458046]
46. Engel MA, Leffler A, Niedermirtl F, Babes A, Zimmermann K, Filipovi MR, Izydorczyk I, Eberhardt M, Kichko TI, Muellertribbensee SM, Khalil M, Siklosi N, Nau C, Ivanoviburmazovi I, Neuhuber WL, Becker C, Neurath MF, and Reeh PW (2011) TRPA1 and substance P mediate colitis in mice. Gastroenterology 141, 1346–1358 [PubMed: 21763243]
47. Liu B, Escalera J, Balakrishna S, Fan L, Caceres AI, Robinson E, Sui A, McKay MC, McAlexander MA, Herrick CA, and Jordt SE (2013) TRPA1 controls inflammation and pruritogen responses in allergic contact dermatitis. FASEB J. 27, 3549–3563 [PubMed: 23722916]
48. Lai NY, Mills K, and Chiu IM (2017) Sensory neuron regulation of gastrointestinal inflammation and bacterial host defence. J. Intern. Med. 282, 5–23 [PubMed: 28155242]
49. Meseguer V, Alpizar YA, Luis E, Tajada S, Denlinger B, Fajardo O, Manenschijn JA, Fernández-Peña C, Talavera A, Kichko T, Navia B, Sánchez A, Señarís R, Reeh P, Pérez-García MT, López-López JR, Voets T, Belmonte C, Talavera K, and Viana F (2014) TRPA1 channels mediate acute neurogenic inflammation and pain produced by bacterial endotoxins. Nat. Commun. 5, 3215 [PubMed: 24477114]
50. Startek JB, Talavera K, Voets T, and Alpizar YA (2018) Differential interactions of bacterial lipopolysaccharides with lipid membranes: implications for TRPA1-mediated chemosensation. Sci. Rep. 8, 12010 [PubMed: 30104600]

51. Chiu IM, Heesters BA, Ghasemlou N, Von Hehn CA, Zhao F, Tran J, Wainger B, Strominger A, Muralidharan S, Horswill AR, Wardenburg JB, Hwang SW, Carroll MC, and Woolf CJ (2013) Bacteria activate sensory neurons that modulate pain and inflammation. Nature 501, 52–57 [PubMed: 23965627]
52. Baral P, Umans BD, Li L, Wallrapp A, Bist M, Kirschbaum T, Wei Y, Zhou Y, Kuchroo VK, Burkett PR, Yipp BG, Liberles SD, and Chiu IM (2018) Nociceptor sensory neurons suppress neutrophil and γδ T cell responses in bacterial lung infections and lethal pneumonia. Nat. Med. 24, 417–426 [PubMed: 29505031]
53. Lin T, Quellier D, Lamb J, Voisin T, Baral P, Bock F, Schönberg A, Mirchev R, Pier G, Chiu I, and Gadjeva M (2021) *Pseudomonas aeruginosa*-induced nociceptor activation increases susceptibility to infection. PLoS Pathog. 17, e1009557 [PubMed: 33956874]
54. Lai NY, Musser MA, Pinho-Ribeiro FA, Baral P, Jacobson A, Ma P, Potts DE, Chen Z, Paik D, Soualhi S, Yan Y, Misra A, Goldstein K, Lagomarsino VN, Nordstrom A, Sivanathan KN, Wallrapp A, Kuchroo VK, Nowarski R, Starnbach MN, Shi H, Surana NK, An D, Wu C, Huh JR, Rao M, and Chiu IM (2020) Gut-innervating nociceptor neurons regulate Peyer's patch microfold cells and SFB levels to mediate Salmonella host defense. Cell 180, 33–49. e22 [PubMed: 31813624]
55. Singer JT, Phennicie RT, Sullivan MJ, Porter LA, Shaffer VJ, and Kim CH (2010) Broad-host-range plasmids for red fluorescent protein labeling of Gram-negative bacteria for use in the zebrafish model system. Appl. Environ. Microbiol. 76, 3467–3474 [PubMed: 20363780]
56. Caterina MJ, Leffler A, Malmberg AB, Martin WJ, Trafton J, Petersen-Zeitz KR, Koltzenburg M, Basbaum AI, and Julius D (2000) Impaired nociception and pain sensation in mice lacking the capsaicin receptor. Science 288, 306–313 [PubMed: 10764638]
57. Bautista DM, Jordt S-E, Nikai T, Tsuruda PR, Read AJ, Poblete J, Yamoah EN, Basbaum AI, and Julius D (2006) TRPA1 mediates the inflammatory actions of environmental irritants and proalgesic agents. Cell 124, 1269–1282 [PubMed: 16564016]
58. Mark Welch JL, Rossetti BJ, Rieken CW, Dewhirst FE, and Borisy GG (2016) Biogeography of a human oral microbiome at the micron scale. Proc. Natl. Acad. Sci. 113, E791–E800 [PubMed: 26811460]
59. Vaishnava S, Yamamoto M, Severson KM, Ruhn KA, Yu X, Koren O, Ley R, Wakeland EK, and Hooper LV (2011) The antibacterial lectin RegIIIγ promotes the spatial segregation of microbiota and host in the intestine. Science (80-.). 334, 255–258
60. Caudle RM, Karai L, Mena N, Cooper BY, Mannes AJ, Perez FM, Iadarola MJ, and Olah Z (2003) Resiniferatoxin-induced loss of plasma membrane in vanilloid receptor expressing cells. Neurotoxicology 24, 895–908 [PubMed: 14637384]
61. Pecze L, Pelsoczi P, Kecskés M, Winter Z, Papp A, Kaszá K, Letoha T, Vizler C, and Oláh Z (2009) Resiniferatoxin mediated ablation of TRPV1+ neurons removes TRPA1 as well. Can. J. Neurol. Sci. 36, 234–241 [PubMed: 19378721]
62. Habib NE, El-Kasaby HT, Marczak AM, and Hsuan J (1993) Subconjunctival bupivacaine versus topical amethocaine in strabismus surgery. Eye 7, 757–759 [PubMed: 8119426]
63. Jinks MR, Fontenot RL, Wills RW, and Betbeze CM (2018) The effects of subconjunctival bupivacaine, lidocaine, and mepivacaine on corneal sensitivity in healthy horses. Vet. Ophthalmol. 21, 498–506 [PubMed: 29232029]
64. Jolly AL, Agarwal P, Metruccio MME, Spiciarich DR, Evans DJ, Bertozzi CR, and Fleiszig SMJ (2017) Corneal surface glycosylation is modulated by IL-1R and *Pseudomonas aeruginosa* challenge but is insufficient for inhibiting bacterial binding. FASEB J. 31, 2393–2404 [PubMed: 28223334]
65. Mergler S, Garreis F, Sahlmüller M, Reinach PS, Paulsen F, and Pleyer U (2011) Thermosensitive transient receptor potential channels in human corneal epithelial cells. J. Cell. Physiol. 226, 1828–1842 [PubMed: 21506114]
66. Blalock TD, Spurr-Michaud SJ, Tisdale AS, Heimer SR, Gilmore MS, Ramesh V, and Gipson IK (2007) Functions of MUC16 in corneal epithelial cells. Investig. Ophthalmol. Vis. Sci. 48, 4509–4518 [PubMed: 17898272]

67. Linden SK, Sutton P, Karlsson NG, Korolik V, and McGuckin MA (2008) Mucins in the mucosal barrier to infection. Mucosal Immunol. 1, 183–197 [PubMed: 19079178]

68. Mantelli F and Argüeso P (2008) Functions of ocular surface mucins in health and disease. Curr. Opin. Allergy Clin. Immunol. 8, 477–483 [PubMed: 18769205]

69. Mochizuki H, Fukui M, Hatou S, Yamada M, and Tsubota K (2010) Evaluation of ocular surface glycocalyx using lectin-conjugated fluorescein. Clin. Ophthalmol. 4, 925–930 [PubMed: 20823935]

70. Hosoi J, Murphy GF, Egan CL, Lerner EA, Grabbe S, Asahina A, and Granstein RD (1993) Regulation of Langerhans cell function by nerves containing calcitonin gene-related peptide. Nature 363, 159–163 [PubMed: 8483499]

71. Reilly CA, Johansen ME, Lanza DL, Lee J, Lim JO, and Yosi GS (2005) Calcium-dependent and independent mechanisms of capsaicin receptor (TRPV1)-mediated cytokine production and cell death in human bronchial epithelial cells. J. Biochem. Mol. Toxicol. 19, 266–275 [PubMed: 16173059]

72. Wan SJ, Ma S, Evans DJ, and Fleiszig SMJ (2020) Resistance of the murine cornea to bacterial colonization during experimental dry eye. PLoS One 15, e0234013 [PubMed: 32470039]

73. Huang LC, Reins RY, Gallo RL, and McDermott AM (2007) Cathelicidin-deficient (Cnlp−/−) mice show increased susceptibility to *Pseudomonas aeruginosa* keratitis. Investig. Ophthalmol. Vis. Sci. 48, 4498–4508 [PubMed: 17898271]

74. Maltseva IA, Fleiszig SMJ, Evans DJ, Kerr S, Sidhu SS, McNamara NA, and Basbaum C (2007) Exposure of human corneal epithelial cells to contact lenses in vitro suppresses the upregulation of human β-defensin-2 in response to antigens of Pseudomonas aeruginosa. Exp. Eye Res. 85, 142–153 [PubMed: 17531223]

75. McNamara NA, Van R, Tuchin OS, and Fleiszig SMJ (1999) Ocular surface epithelia express mRNA for human beta defensin-2. Exp. Eye Res. 69, 483–490 [PubMed: 10548468]

76. Haynes RJ, Tighe PJ, and Dua HS (1998) Innate defence of the eye by antimicrobial defensin peptides. Lancet 352, 451–452

77. Cavanaugh DJ, Chesler AT, Jackson AC, Sigal YM, Yamanaka H, Grant R, O'Donnell D, Nicoll RA, Shah NM, Julius D, and Basbaum AI (2011) TRPV1 reporter mice reveal highly restricted brain distribution and functional expression in arteriolar smooth muscle cells. J. Neurosci. 31, 5067–5077 [PubMed: 21451044]

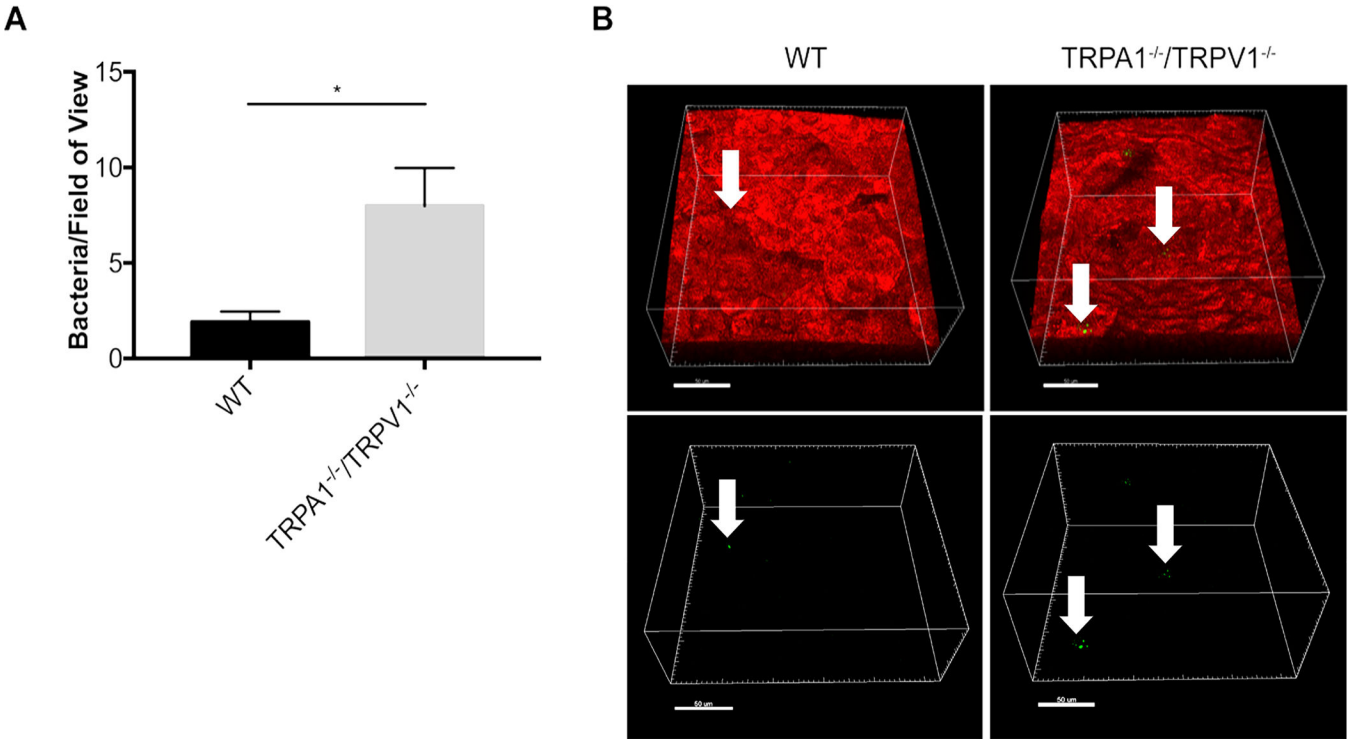

Figure 1.

FISH reveals increased adhesion of environmental bacteria on corneas of TRPA1$^{-/-}$/TRPV1$^{-/-}$ mice compared to wild-type (WT). **A.** Quantification of bacteria detected on healthy corneas of WT versus TRPA1$^{-/-}$/TRPV1$^{-/-}$ by FISH labeling using a universal 16S rRNA gene probe (~ 4-fold difference). Data are expressed as the mean ± SEM number of bacteria per field of view (area of 211μm by 211μm). * $P < 0.05$ (Student's t-Test). **B.** Representative confocal images showing FISH labeling (green, arrows) of environmental bacteria on WT and TRPA1$^{-/-}$/TRPV1$^{-/-}$ corneas. Upper panels show bacteria (arrows) in the context of the cell membranes of *mT/mG* mice (red). Lower panels show the same bacteria (green) without cell membrane fluorescence. Scale bar = 50 μm.

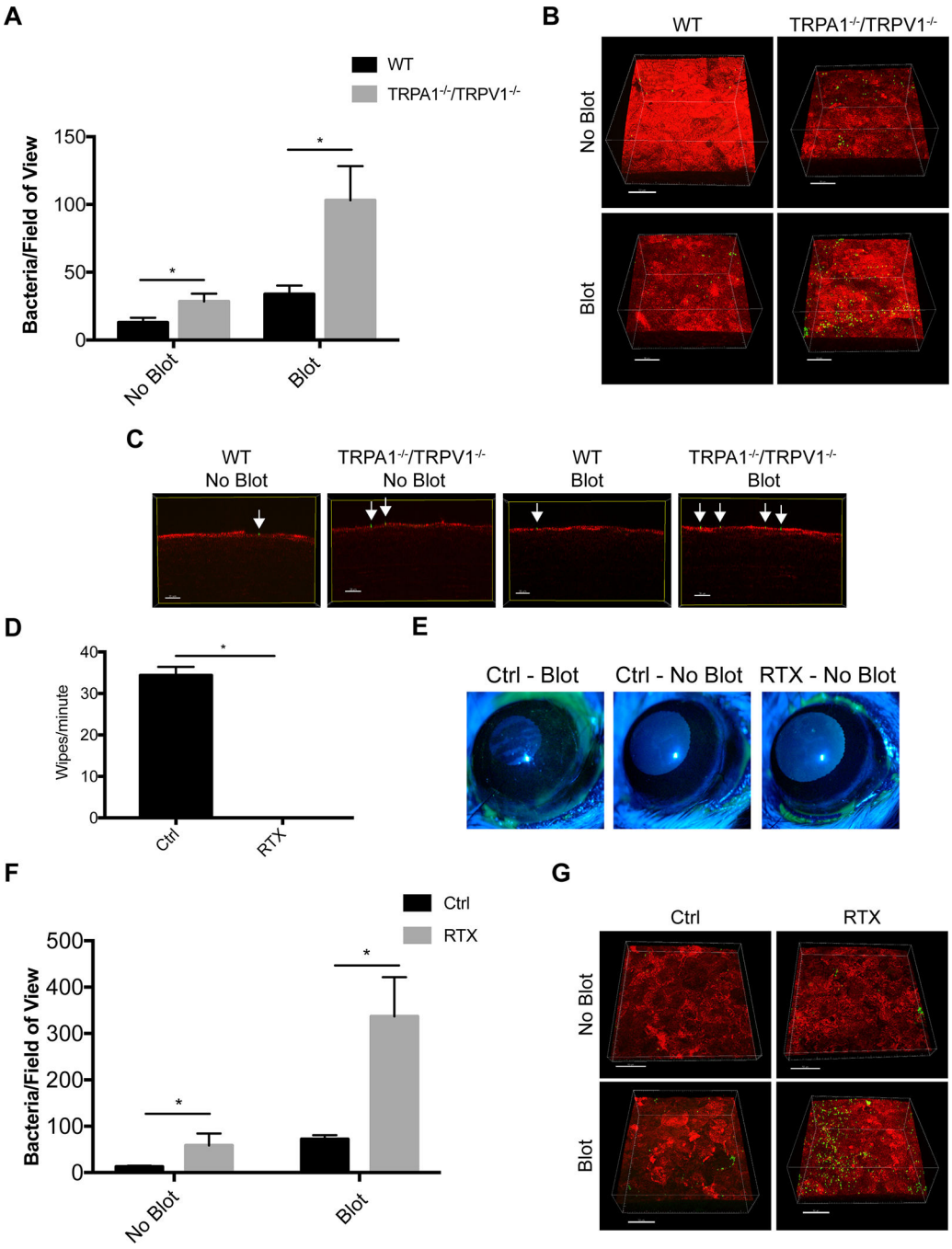

Figure 2.

Inoculated *P. aeruginosa* shows significantly greater adhesion to mouse corneas lacking TRPA1 and TRPV1 nociceptors compared to controls. **A.** Quantification of bacteria adhering to murine corneas per field of view after inoculation of ~ 1×10^{11} CFU/mL every hour for 4 h on both intact (no blot) and tissue-paper blotted corneas. $TRPA1^{-/-}$/$TRPV1^{-/-}$ corneas showed significantly greater bacterial adhesion than WT (~ 2.2-fold) with blotting causing a greater difference from WT (~ 3.1-fold). Data are expressed as the mean ± SEM number of bacteria per field of view. * $P < 0.05$ (Two-way ANOVA). **B.**

Representative images of *P. aeruginosa* (green) adhering to the murine cornea (red) under each condition. Scale bar = 50 μm. **C.** Optical slices of the XZ axis showing that bacteria remained surface-associated (green, arrows) and did not penetrate the corneal epithelium (red). Scale bar = 20 μm. **D**. Quantification of eye wipes over 1 min after capsaicin (100 μM) was dropped onto lightly anesthetized control and RTX-treated mice. RTX-treated mice did not wipe their eyes after capsaicin application versus controls (mean of 34 wipes/min). * $P < 0.05$ (Mann-Whitney U Test). **E.** Corneal fluorescein staining observed by slit lamp examination in blotted control eyes compared to the absence of staining in intact (no blot) control or RTX-treated corneas indicating normal epithelial integrity. **F.** Quantification of bacteria adhering to corneas of RTX-treated mice versus WT controls after 4 h of *P. aeruginosa* inoculation. Intact corneas (no blot) of RTX-treated mice showed significantly greater adhesion than WT (~ 3.7-fold). After blotting, a greater difference was observed between RTX-treated mice and WT (~ 4.7-fold). Data are expressed as the mean ± SEM number of bacteria per field of view. * $P < 0.05$ (Two-way ANOVA). **G.** Representative images of *P. aeruginosa* (green) adhering to the murine cornea (red) under each condition. Scale bar = 50 μm.

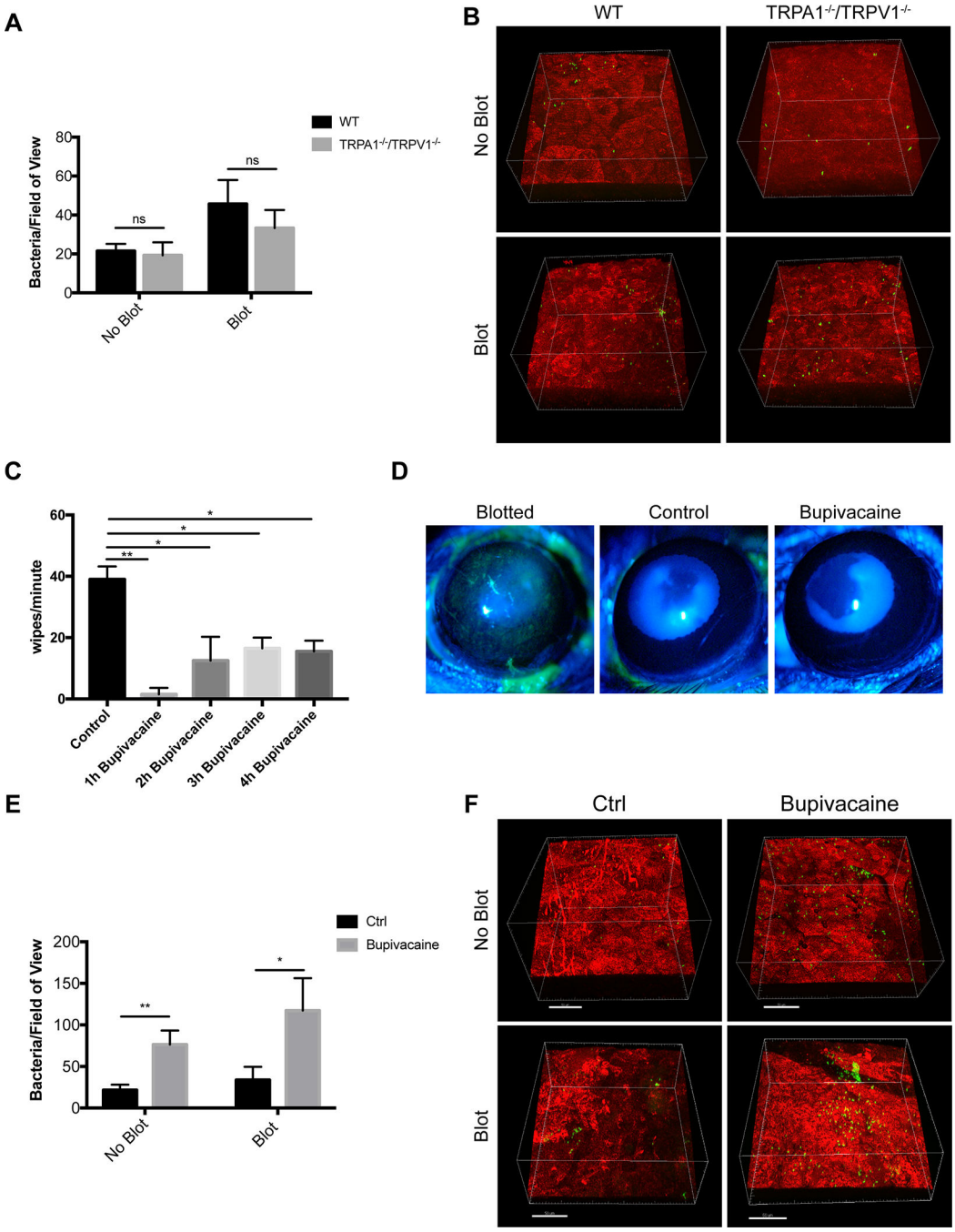

Figure 3.

Evidence for corneal nerve involvement in preventing *P. aeruginosa* adhesion to the murine cornea. **A.** Quantification of bacteria adhering to the murine cornea *ex vivo* after inoculation with ~1×10^{11} CFU/mL *P. aeruginosa* on healthy (no blot) and blotted corneas. *Ex vivo*, equal numbers of *P. aeruginosa* adhered to TRPA1$^{-/-}$/TRPV1$^{-/-}$ corneas compared to WT under both healthy and blotted conditions after 4 h. More bacteria adhered to blotted corneas as expected. ns = not significant (Two-way ANOVA). **B.** Representative images of *P. aeruginosa* (green) adhering to the cornea (red) in each condition. **C.** Bupivacaine-treated

WT mice showed a significantly diminished response to capsaicin lasting for 4 h compared to mice treated with vehicle control. * $P < 0.05$, ** $P < 0.01$ (One-way ANOVA with Tukey's multiple comparisons test). **D.** Fluorescein staining of a blotted WT mouse cornea under the slit lamp. Staining was absent in WT mouse corneas treated with either vehicle control or bupivacaine indicating normal epithelial integrity. **E.** Bupivacaine-treated WT mouse corneas *in vivo* showed significantly increased adhesion by *P. aeruginosa* versus vehicle controls under healthy (~ 3.6-fold) and blotted (~ 3.5-fold) conditions. * $P < 0.05$, ** $P < 0.01$ (Two-way ANOVA). **F.** Representative images of *P. aeruginosa* (green) adhering to the cornea (red) in control and bupivacaine-treated mice. Scale bar = 50 μm.

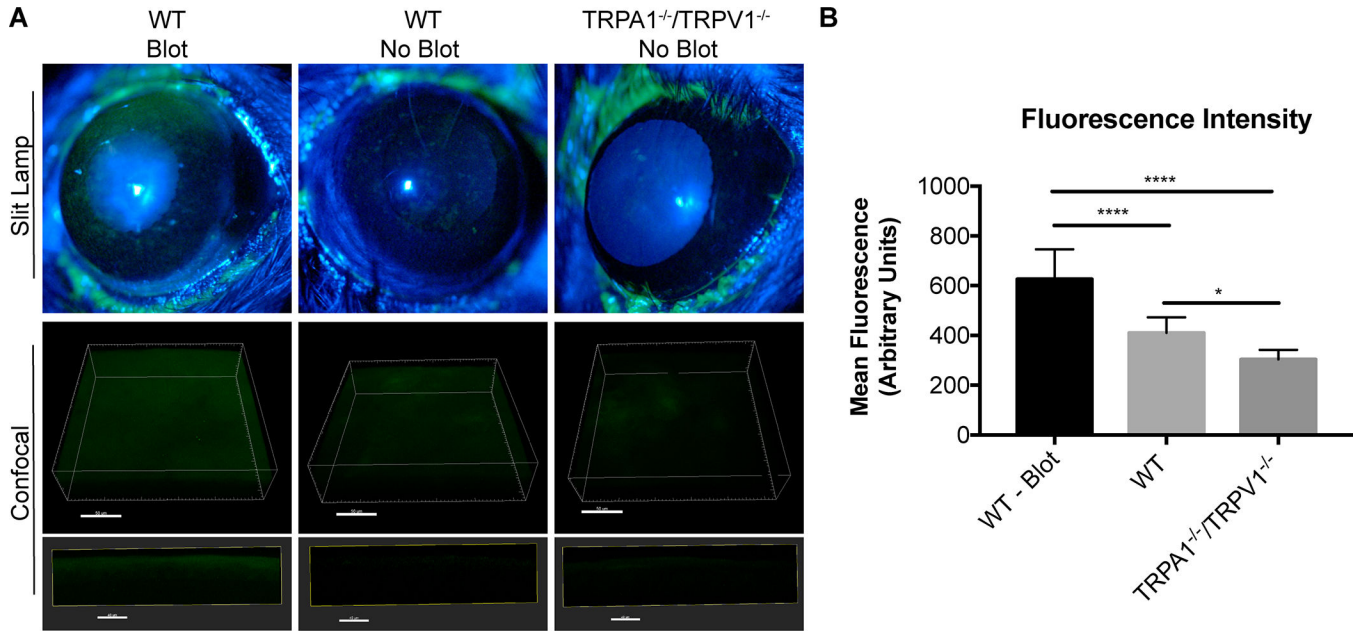

Figure 4.

Intact TRPA1$^{-/-}$/TRPV1$^{-/-}$ mouse corneas do not stain with fluorescein. **A.** Fluorescein staining under a slit lamp (upper panels) was evident in blotted corneas of WT mice but absent in healthy corneas (no blot) of WT and TRPA1$^{-/-}$/TRPV1$^{-/-}$ mice. Confocal images (lower panels) also show that healthy (no blot) corneas of TRPA1$^{-/-}$/TRPV1$^{-/-}$ and WT mice have little fluorescein staining (and no fluorescein penetration) indicating epithelial integrity was intact compared to blotted WT positive controls. Upper confocal panel images are 3D reconstructions of corneal images (Scale bar = 50 μm) and lower confocal panel images are 10 μM XZ stacks (Scale bar = 40 μm). **B.** Quantification of mean fluorescence intensity of fluorescein staining in Z-projection of confocal images. Data expressed as the mean ± SEM. **** $P < 0.0001$, * $P < 0.05$ (One-way ANOVA with Tukey's multiple comparisons test).

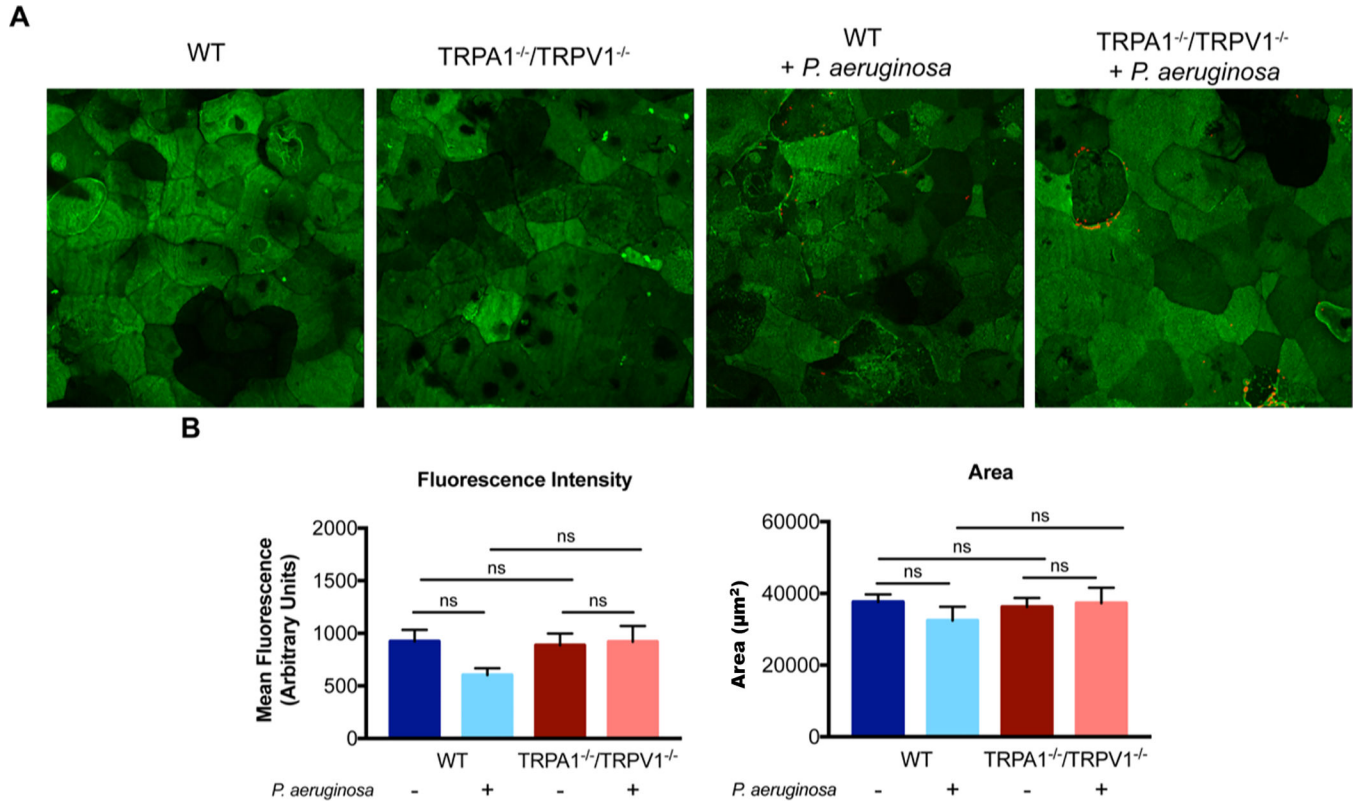

Figure 5.

Wheat germ agglutinin (WGA) labeling of TRPA1$^{-/-}$/TRPV1$^{-/-}$ mouse corneas is similar to wild-type. **A.** Representative maximum intensity projections of WGA labeling (green) and *P. aeruginosa* adhesion (red) to the intact epithelium (i.e. no tissue paper blotting) of wild-type and TRPA1$^{-/-}$/TRPV1$^{-/-}$ corneas. Similar WGA labeling was observed across all conditions, and *P. aeruginosa* adherence (red) can be observed in TRPA1$^{-/-}$/TRPV1$^{-/-}$ corneas. **B.** Quantification of WGA mean fluorescence intensity and area of WGA labeling. No significant differences were observed for either measurement between WT or TRPA1$^{-/-}$/TRPV1$^{-/-}$ mice with or without inoculation with *P. aeruginosa* indicating a normal epithelial surface and response to bacteria. Data are expressed as the mean ± SEM. ns = Not Significant (One-way ANOVA with Tukey's multiple comparisons test).

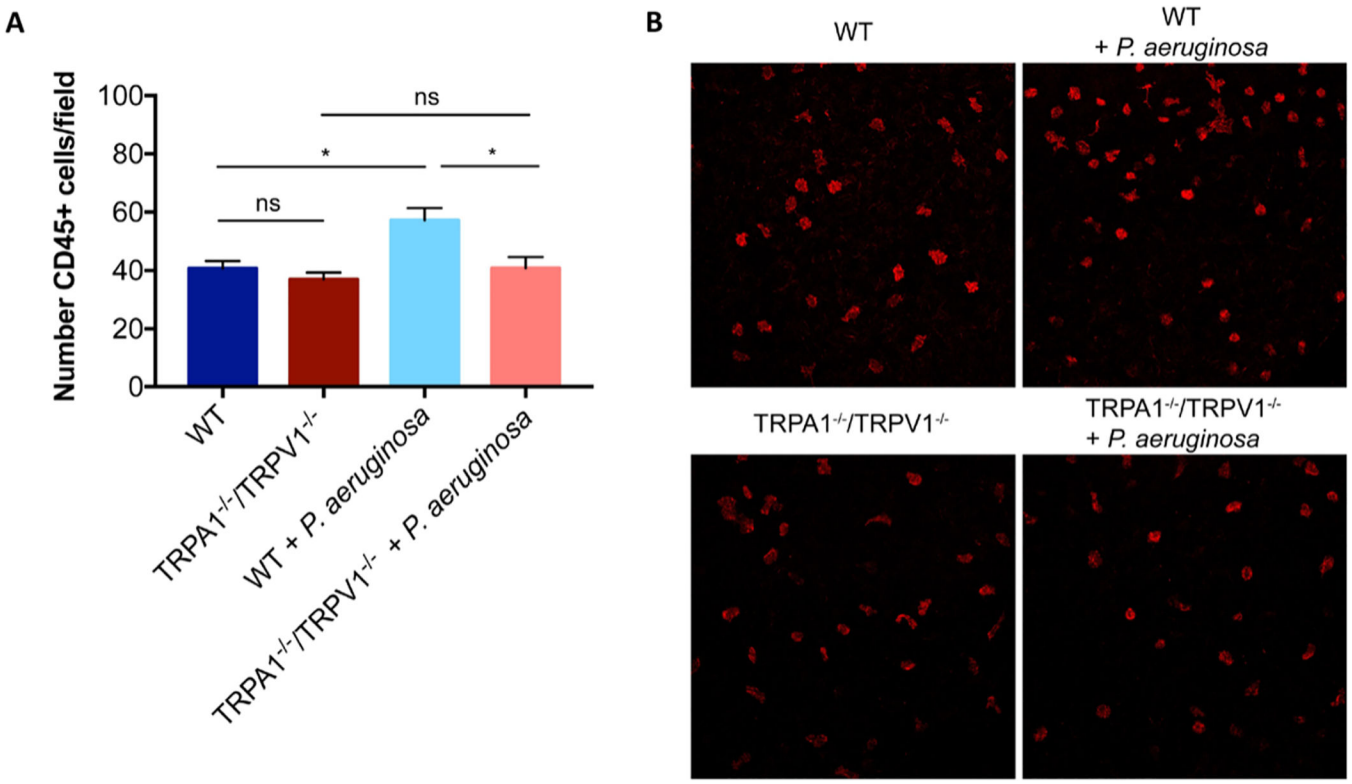

Figure 6.

TRPA1$^{-/-}$/TRPV1$^{-/-}$ corneas show reduced CD45+ cell infiltration after bacterial challenge compared to WT mice. **A**. Quantification of CD45+ cells in healthy (untreated) corneas of control and TRPA1$^{-/-}$/TRPV1$^{-/-}$ mice at baseline and at 4 h after *P. aeruginosa* challenge. A significant increase in CD45+ cells was observed after *P. aeruginosa* inoculation in control mice that was not observed in TRPA1$^{-/-}$/TRPV1$^{-/-}$ mice. * $P < 0.05$, ns = Not Significant (One-way ANOVA with Tukey's multiple comparisons test). **B.** Representative images (maximum intensity projections) of CD45+ cells in the central murine cornea in each condition. Scale bar = 50 μm.

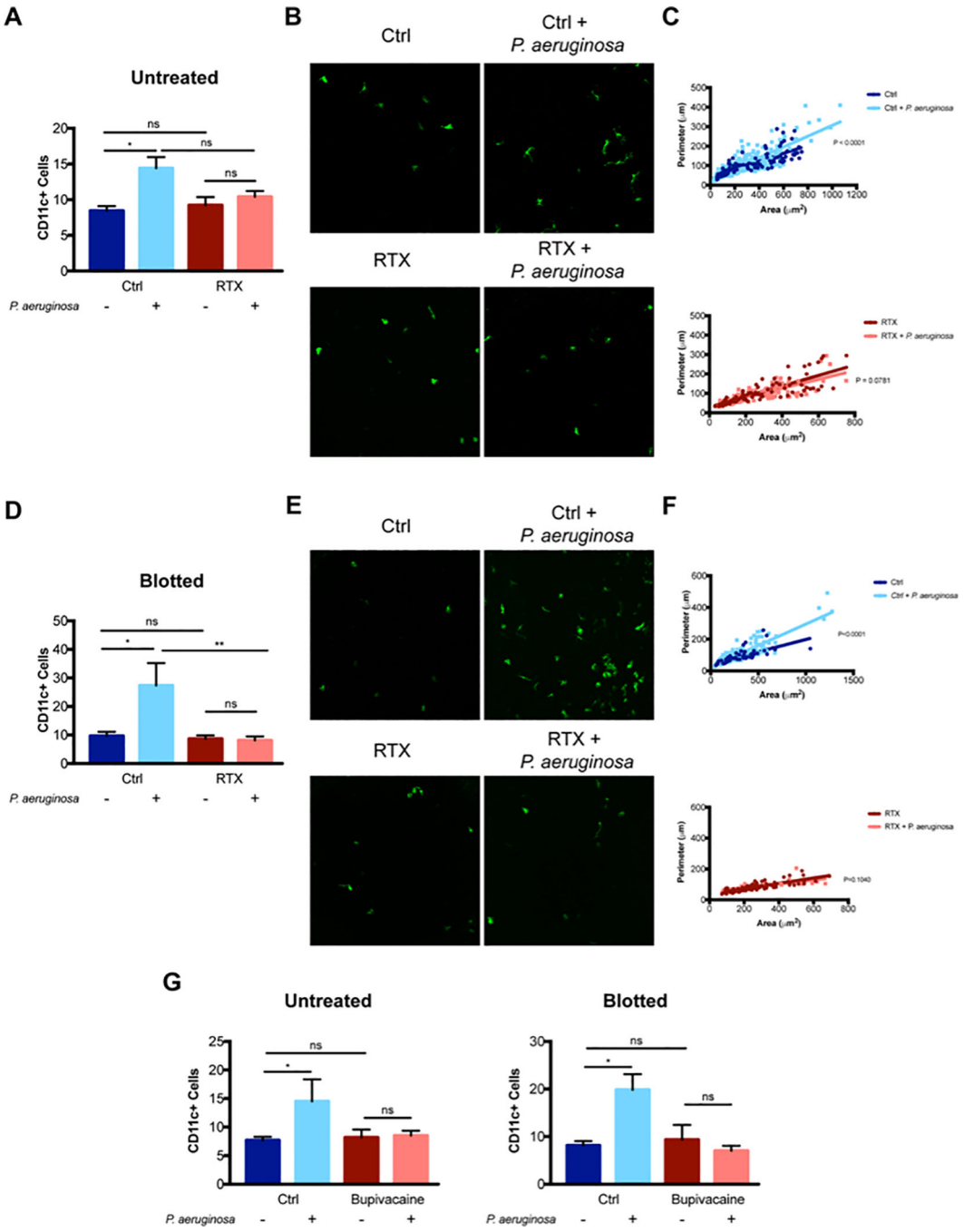

Figure 7.

RTX and bupivacaine attenuate CD11c+ cell infiltration of the murine cornea in response to *P. aeruginosa*. **A.** Quantification of CD11c+ cells in healthy (untreated) corneas of control and RTX-treated CD11c-YFP mice at baseline and at 4 h after *P. aeruginosa* challenge. A significant increase in CD11c+ cells was observed after *P. aeruginosa* inoculation in control mice that was not observed in RTX-treated mice. * $P < 0.05$, ns = Not Significant (One-way ANOVA with Tukey's multiple comparisons test). **B.** Representative images (maximum intensity projections) of CD11c+ cells in the murine cornea in each condition.

C. Morphological analysis of CD11c+ cells using MorpholibJ tools for 3D segmentation in ImageJ and parameters related to z-projections used (perimeter and area) to exclude artifacts due to lower z resolution. Graphs show the distribution of individual cells based on their area and perimeter with a linear regression fit. The upper panel shows a significant difference between curves ($P < 0.0001$) in control mice with *P. aeruginosa* inoculation causing increased cell perimeter. The lower panel shows no significant difference between curves ($P = 0.078$) after *P. aeruginosa* inoculation in RTX-treated mice. **D.** Quantification of CD11c+ cells in blotted corneas of control and RTX-treated CD11c-YFP mice at baseline and at 4 h after *P. aeruginosa* challenge. A significant increase in CD11c+ cells was observed after *P. aeruginosa* inoculation in controls that was not observed in RTX-treated mice. * $P < 0.05$, ** $P < 0.01$, ns = Not Significant (One-way ANOVA with Tukey's multiple comparisons test). **E.** Representative images (maximum intensity projections) of CD11c+ cells in blotted corneas in each condition. **F.** Morphological analysis of blotted corneas showed a significant difference between curves ($P < 0.0001$) in controls with *P. aeruginosa* inoculation causing increased cell perimeter, but no difference in curves ($P = 0.104$) in blotted RTX-treated corneas after *P. aeruginosa* inoculation. **G.** Quantification of corneal CD11c+ cells in control and bupivacaine treated mice at baseline and after *P. aeruginosa* inoculation for 4 h for healthy (untreated) and blotted corneas. For both untreated and blotted corneas, *P. aeruginosa* inoculation caused a significant increase in CD11c+ cells. Bupivacaine treated corneas showed no response to bacteria. * $P < 0.05$, ns = Not Significant (One-way ANOVA with Tukey's multiple comparisons test).

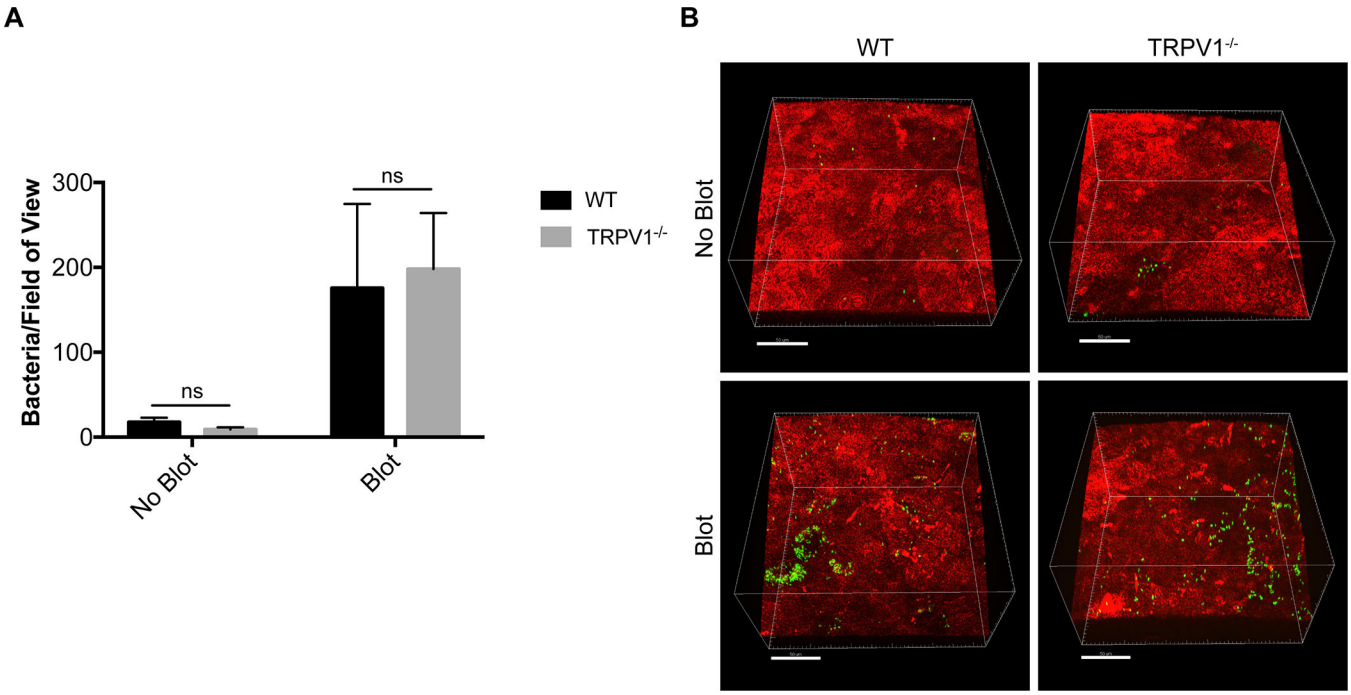

Figure 8.

TRPV1$^{-/-}$ corneas show similar bacterial adhesion to WT *in* vivo. **A**. Quantification of *P. aeruginosa* adhesion to healthy and blotted murine corneas after inoculation of ~1×10^{11} CFU/mL every hour for 4 h. Under each condition, there was no significant difference in bacterial adhesion between TRPV1$^{-/-}$ corneas and WT. As expected, more bacteria adhered to blotted corneas. ns = Not Significant (Two-way ANOVA). **B**. Representative images of *P. aeruginosa* (green) adhering to the murine cornea (red) in each condition. Scale bar = 50 μm.

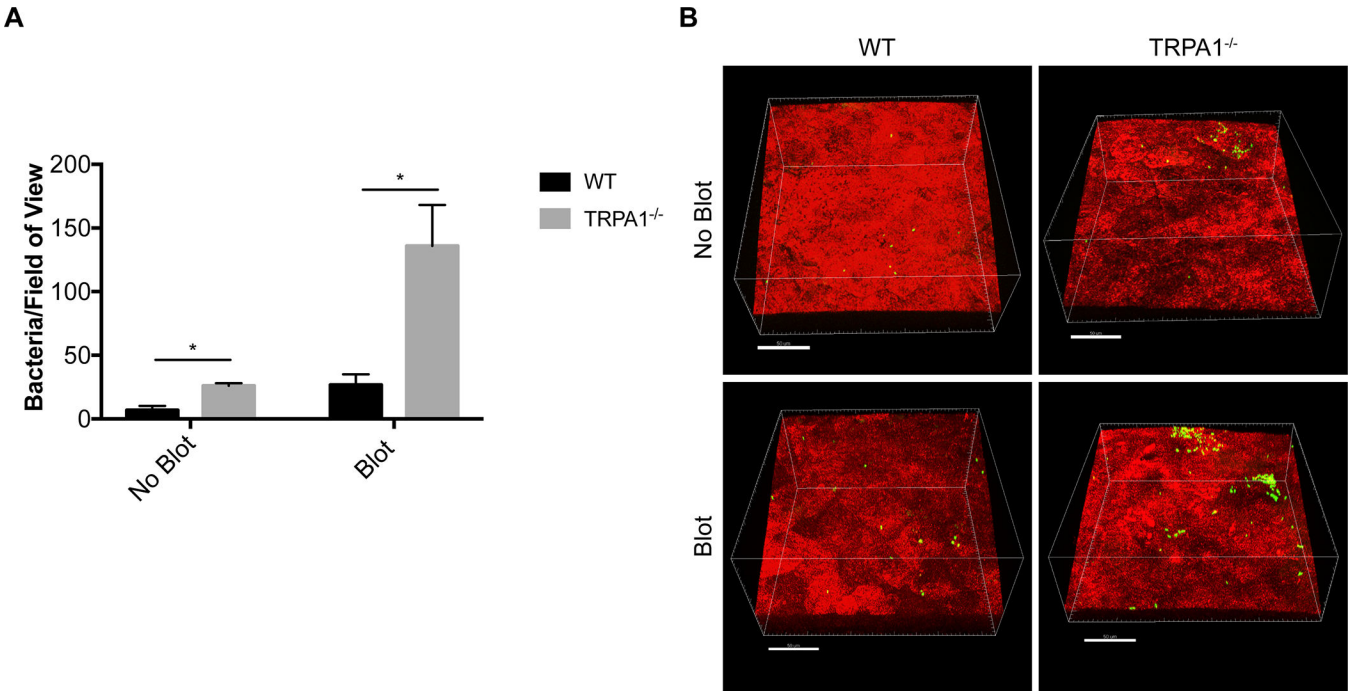

Figure 9.

TRPA1$^{-/-}$ corneas show significantly greater bacterial adhesion compared to WT *in vivo.* **A**. Quantification of bacterial adhesion to healthy and blotted murine corneas after inoculation of ~1×10^{11} CFU/mL every hour for 4 h comparing TRPA1$^{-/-}$ mice to WT. Healthy TRPA1$^{-/-}$ corneas showed ~3.8-fold greater adhesion than WT, and blotted TRPA1$^{-/-}$ corneas showed a ~5.1-fold increase over WT. * $P < 0.05$ (Two-way ANOVA). **B.** Representative images of *P. aeruginosa* (green) adhering to the murine cornea (red) in each condition. Scale bar = 50 μm.

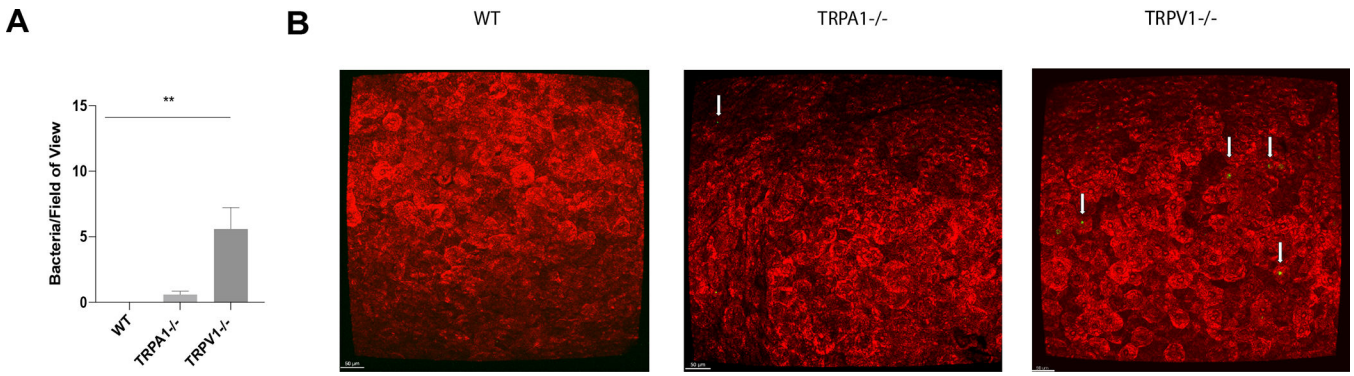

Figure 10.

FISH reveals increased adhesion of environmental bacteria on healthy corneas of TRPV1$^{-/-}$ mice compared to WT and TRPA1$^{-/-}$ mice. **A.** Quantification of viable bacteria detected on healthy corneas of WT (none detected), TRPA1$^{-/-}$ (1 ± 1 bacteria/field of view) and TRPV1$^{-/-}$ (6 ± 4 bacteria/field of view) by FISH labeling using a universal 16S rRNA gene probe. Data are expressed as the mean ± SEM (area of 1600 μm by 1600 μm). ** P < 0.005 (Two-way ANOVA), WT vs. TRPA1−/− was not significant (Two-Way ANOVA). **B.** Representative confocal images of WT, TRPA1$^{-/-}$ and TRPV1$^{-/-}$ corneas (red) after FISH labeling of any environmental bacteria detected (green, arrows). Scale bar = 50 μm.